20266-6006-RO-00

MONOPROPELLANT HYDRAZINE RESISTOJET

ANALYSIS TASK SUMMARY REPORT

TRW SYSTEMS GROUP
1 SPACE PARK
REDONDO BEACH, CALIFORNIA 90278

NOVEMBER 1971

PREPARED FOR
GODDARD SPACE FLIGHT CENTER
GREENBELT, MARYLAND 20771

TRW
SYSTEMS GROUP

20266-6006-R0-00

MONOPROPELLANT HYDRAZINE RESISTOJET

ANALYSIS TASK SUMMARY REPORT

TRW SYSTEMS GROUP
1 SPACE PARK
REDONDO BEACH, CALIFORNIA 90278

NOVEMBER 1971

PREPARED FOR
GODDARD SPACE FLIGHT CENTER
GREENBELT, MARYLAND 20771

Prepared by F. B. Muenzer

Approved by

C.K. Murch
Project Manager
TRW Systems

D. Asato
Technical Officer
NASA/Goddard Space Flight Center

TRW
SYSTEMS GROUP

FOREWORD

This is the first Task Summary Report submitted under Contract NAS5-11477, "Design, Development, and Testing of Engineering Model 20-Millipound Thrust Monopropellant Hydrazine Resistojet." The program originated in the Auxiliary Propulsion Branch of the NASA/Goddard Space Flight Center. Mr. Dennis Asato is the Technical Officer for the NASA/GSFC. Mr. Charles K. Murch is the Project Manager for TRW Systems Group. The primary contributor to this report was Mr. Frank B. Muenzer.

Table of Contents

Table of Contents (Continued)

LIST OF FIGURES

LIST OF FIGURES (Continued)

1.0 SUMMARY

The analysis tasks for the Electrothermal Hydrazine Thruster (EHT) Program are intended to provide mathematical models which can be utilized to aid in preliminary design definition, interpretation of test data, and the evaluation of design and operational changes. Within the scope of these requirements, three computer programs were formulated to provide the necessary steady-state and transient performance design tools. These included:

1. A program to provide preliminary evaluation of the energy balance characteristics of the thruster.
2. A program to provide a means of evaluating steady-state performance relative to the primary design, configuration, and operational parameters.
3. A model to provide a means of evaluating transient (pulse mode) operation of the thruster relative to primary design and operational parameters.

The steady-state energy balance and performance programs for the Electrothermal Hydrazine Thruster were formulated on the TRW Timeshare Digital System to provide a tabular data printout. The transient performance model was formulated on a C15000 active-element analog computer to provide direct time variant output of the predicted operational characteristics.

Parameter studies were conducted with both the analog computer transient model and the digital steady-state program. Studies included evaluation of the effects on thruster operation of variations in supply pressure, percent ammonia dissociation, wall and screen pack surface area, thruster volumes (head-end and chamber), thruster mass, electrical power, holding temperature, throat and injector area, and nozzle thrust coefficient. Thruster performance parameters included: impulse, specific impulse, characteristic velocity, thrust coefficient, wall and chamber temperature, thrust, and flowrate as well as internal pressures and temperatures.

Included in this report are: a discussion of the analytical models, including the flow schematics and program listings; tabulated data from the parameter studies with typical program output data; and a discussion of the study results.

2.0 ANALYTICAL MODELS

2.1 Discussion

While essentially three separate analytical models were formulated, the energy balance computer model served primarily as a preliminary aid in understanding the thruster energy balance. This model was effectively replaced as an evaluation tool by the more extensive steady-state and transient performance models. For the sake of completeness, however, discussions of all three models are included in this report.

It should be noted that both the steady-state and transient performance models are based on a lumped parameter representation of the Electrothermal Hydrazine Thruster. By this method, the pressure, flowrate, heat transfer and other characteristics of the thruster (shown schematically in Figure 2-1) are analytically described as occurring at a finite number of specified nodes. Thus, the pressure/flow characteristics, for example, are schematically represented as shown in Figure 2-2. In this figure, R_1, R_2, R_3, and R_4, represent the valve flow resistance, injector flow resistance, screen pack flow resistance, and nozzle throat flow resistance. P_0 represents the supply pressure, and the capacitance effects at P_1, P_2, and P_3 determine the injector inlet pressure, head end pressure, and chamber pressure, respectively.

For all of the studies summarized here, a nominal configuration was defined as follows:

Injector flow area	=	$4.48(10^{-6})$ in^2
Head End Volume	=	0.059 in^3
Chamber Volume	=	0.059 in^3
Throat Area	=	$3.14(10^{-4})$ in^2
Thruster Weight	=	0.0146 lb

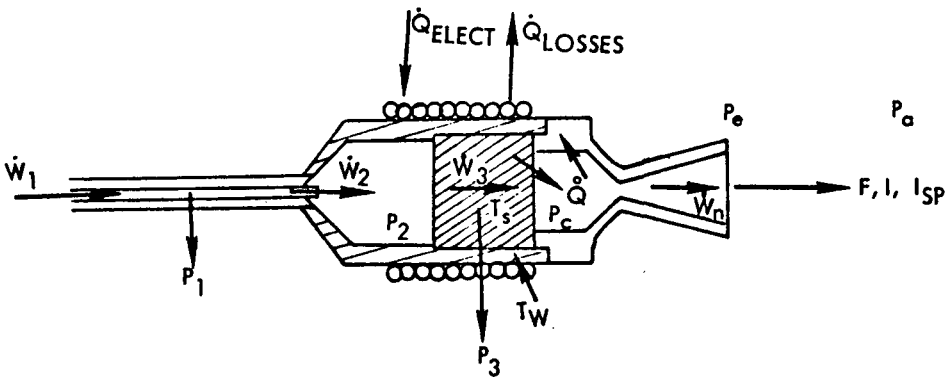

Figure 2-1 ELECTROTHERMAL HYDRAZINE THRUSTER SCHEMATIC

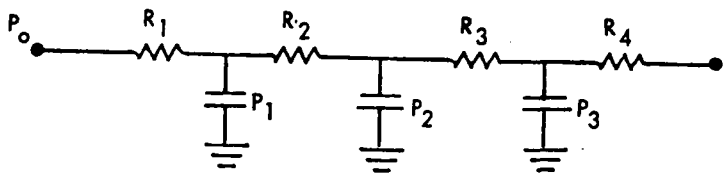

Figure 2-2 LUMPED PARAMETER PRESSURE/FLOW SCHEMATIC OF ELECTOTHERMAL HYDRAZINE THRUSTER

2.2 Energy Balance Analysis

2.2.1 Introduction

The energy balance analysis was conducted to provide a general understanding of the nominal energy distribution and performance characteristics for specified thruster operating conditions. In order to provide this preliminary evaluation, an analytical model was formulated and a digital computer program written to provide a rapid iterative solution to the equations.

In operation, program inputs required are chamber pressure, throat area, electrical power, thermal losses, propellant inlet temperature and nozzle C_f. Specific heat ratio (γ) and specific heat (C_p) are defined as a function of dissociation fraction (from Reference 1). Based on these values, program calculations and output include: chamber temperature, flowrate, thrust, specific impulse, net decomposition and dissociation energy. The typical program output is illustrated in Figure 2-3 and the program listing (designated as program "Frank") is included in the appendix of this report. The analytical model is summarized in Section 2.2.2.

2.2.2 Analytical Model-Energy Balance Program

The thermal decomposition of hydrazine may be assumed to occur in two stages, decomposition and dissociation (see Reference 1), thus

$$3N_2H_4 \rightarrow 4NH_3 + N_2 + 144,300 \text{ BTU} \qquad \text{exothermic decomposition}$$

and

$$4NH_3 \rightarrow 2N_2 + 6H_2 - 79,200 \text{ BTU} \qquad \text{endothermic dissociation}$$

converting from lb/mol to lbm mass units, it may be shown that

(1) Q_{c_1} = (net exothermic reaction heat) = 1505 BTU/lb

and

(2) Q_D = (heat of dissociation) = 825 X BTU/lb

where X = percent dissociation of ammonia.

FIGURE 2-3

TYPICAL ENERGY BALANCE PROGRAM OUTPUT

Conditions: Electrical input, $\dot{Q}_1$ = 12 watts

Chamber pressure, P_c = 76.79 psi

Thrust Coefficient, C_f = 1.654

Losses = 5.41 watts

```
? PC=76.79,QDOT1=12.,QDOTL=5.41,CF=1.654$

    CHAMBER PRESSURE     =  7.679E+01  PSIA
    THROAT AREA          =  3.140E-04  INCHES SQUARE
    CHAMBER TEMPERATURE  =  2.566E+03  DEGREES R
    INLET TEMPERATURE    =  5.300E+02  DEGREES R
    FLOWRATE             =  1.760E-04  LBS./SEC.
    SPECIFIC IMPULSE     =  2.266E+02  SEC.
    THRUST               =  3.988E-02  LBS.-F

                          BTU/SEC       WATTS
  ELECTRICAL INPUT =  1.138E-02     1.200E+01
  DECOMPOSITION    =  2.649E-01     2.793E+02
* VAPORIZATION     =  0.            0.
  DISSOCIATION     =  4.356E-02     4.592E+01
  LOSSES           =  5.132E-03     5.410E+00
```

* As indicated in equation 6, Vaporization heat is assumed to be included in the 1505 BTU/lb of available energy.

For the Electrothermal Hydrazine Thruster, the temperature of the gas in the combustion chamber may be defined by

$$(3)\quad T_c = T_v + \Delta T$$

where T_v = vapor temperature, (propellant is assumed to vaporize in thruster head end)

and ΔT = temperature increase resulting from the decomposition/dissociation reactions.

Also,

$$(4)\quad C_p \dot{w} \Delta T = \sum \dot{Q}$$

where C_p = specific heat of gas

$\dot{w}$ = mass flowrate, lb/sec

$\sum \dot{Q}$ = sum of heat input and losses (including external power, thermal energy losses, etc.)

or

$$(5)\quad C_p \dot{w} \Delta T = (Q_c - C_p(T_v - T_1) - H - Q_D)\, \dot{w} - \dot{Q}_L + \dot{Q}_E$$

where Q_c = decomposition reaction heat input, BTU/lb

T_1 = propellant inlet temperature, °F

H = latent heat of vaporization, BTU/lb

Q_D = endothermic reaction heat loss, BTU/lb

$\dot{Q}_L$ = heat losses, BTU/sec

$\dot{Q}_E$ = electrical heat input, BTU/sec

From Equations 1 and 2 (Reference 1) we have

$$(6)\quad Q_c - C_p\,(T_v - T_1) - H = 1505 \text{ BTU/lb}$$

and

$$(7)\quad Q_D = 825 \text{ X BTU/lb}$$

So

$$(8)\quad C_p \dot{w} \Delta T = (1505 - 825X)\,\dot{w} - \dot{Q}_L + \dot{Q}_E$$

Now, since the relationship between thrust, flowrate and specific impulse is

$$(9)\quad I_{sp} = \frac{F}{\dot{w}}$$

where thrust is defined by

$$(10)\quad F = C_f P_c A_t$$

and nozzle flowrate by

$$(11)\quad \dot{w} = \frac{A_t P_c}{\sqrt{RT_c}} \sqrt{g\gamma \left(\frac{2}{\gamma+1}\right)^{\frac{\gamma+1}{\gamma-1}}}$$

where F = thrust, lbf

C_f = nozzle thrust coefficient

A = nozzle throat area, in^2

R = gas constant = $\frac{(\gamma-1)}{\gamma} C_p$ (C_p = gas specific heat)

γ = gas specific heat ratio

Thus, substituting for $\dot{w}$ and F.

$$(12)\quad I_{sp} = \frac{C_f \sqrt{RT_c}}{\sqrt{\gamma g \left(\frac{2}{\gamma+1}\right)^{\frac{\gamma+1}{\gamma-1}}}}$$

In the above equation, γ and C_p are functions of X (percent ammonia dissociation).

2.3 Steady-State Analysis

2.3.1 Introduction

The steady-state performance model was formulated to provide a more accurate assessment of thruster steady-state operation relative to design parameters such as chamber size, injection pressure drop, nozzle configuration, screen pack pressure drop and heat transfer area as well as supply pressure and temperature, thruster holding power, and thermal losses. This model was utilized to conduct parametric sensitivity and design variation studies to define the

effects of the above parameters on chamber temperature, specific impulse, characteristic velocity, and thrust of the Electrothermal Hydrazine Thruster.

The program input parameters and calculated performance variables are summarized in the typical output data shown in Figure 2-4. A complete program listing is included in Section 5.0. The analytical model is summarized in Section 2.3.2.

```
                    ***INPUTS***

SUPPLY PRESSURE            =  2.000E+02  PSIA.
SUPPLY TEMPERATURE         =  7.000E+01  DEGREES F
ELECTRICAL POWER INPUT     =  1.200E+01  WATTS
DISSOCIATION FRACTION      =  3.000E-01
INJECTOR AREA              =  4.480E-06  SQUARE INCHES
THROAT AREA                =  3.140E-04  SQUARE INCHES
EXPANSION RATIO            =  5.000E+01

                    ---OUTPUT---

INJECTOR INLET PRESSURE          =  1.372E+02  PSIA
HEAD END PRESSURE                =  8.016E+01  PSIA
AVERAGE SCREEN PACK PRESSURE     =  7.848E+01  PSIA
CHAMBER PRESSURE                 =  7.681E+01  PSIA

VAPORIZATION TEMPERATURE  =  3.360E+02  DEGREES F
AVERAGE GAS TEMPERATURE   =  1.590E+03  DEGREES F
SCREEN PACK TEMPERATURE   =  1.590E+03  DEGREES F
WALL TEMPERATURE          =  1.595E+03  DEGREES F
CHAMBER TEMPERATURE       =  2.106E+03  DEGREES F

CHEMICAL HEAT INPUT       =  2.332E+02  WATTS
WALL TO SCREEN HEAT FLUX  =  7.926E-01  WATTS
WALL TO GAS HEAT FLUX     =  5.976E+00  WATTS
SCREEN TO GAS HEAT FLUX   =  7.926E-01  WATTS
HEAT LOSSES               =  5.231E+00  WATTS

THRUST COEFFICIENT  =  1.654E+00
FLOWRATE            =  1.759E-04  LBS./SEC.
THRUST              =  3.988E-02  LBS.-F
SPECIFIC IMPULSE    =  2.268E+02  SEC.
CSTAR               =  4.415E+03  FT/SEC.
```

Figure 2-4 Typical Steady-State Computer Program Output

2.3.2 Analytical Model

The steady-state thruster flow model is as follows:

Liquid valve flowrate is defined by

$$(13)\quad \dot{w} = C_D A_v \left[2\, g\rho\, (P_o - P_1) \right]^{1/2}$$

Since at steady-state, the valve, injector, screen pack and nozzle flowrates are all the same, the injector inlet pressure, P_1, is defined by

$$(14)\quad P_1 = \frac{\dot{w}^2}{2g\rho C_D^{\,2} A_i^2} + P_2$$

and chamber pressure (P_c) by

$$(15)\quad P_c = P_2 - \frac{\dot{w}^2 R T_3}{P_3 K_i}$$

where

$$(16)\quad P_3 = \frac{P_2 + P_c}{2}$$

Further, the nozzle flowrate must also satisfy (for a correct steady-state solution)

$$(17)\quad \dot{w}_n = \frac{P_c A_t g}{C^*}$$

For the above equations

C_D = valve flow coefficient

A_v = Valve flow area, in^2

C^* = gas characteristic velocity, ft/sec

g = constant, ft/sec^2

ρ = liquid hydrazine density, lb/in^3

P_o = supply pressure, lb/in^2

P_2 = head-end pressure, lb/in^2

A_i = injector flow area, in^2

k_i = screen pack pressure drop coefficient, in^5/sec^2

A_t = nozzle thrust area, in^2

T_3, P_3 = average temperature and pressure in screen pack, °R, lb/in^2

The thermodynamics of the steady-state model are defined by

$$(18)\quad \dot{Q}_o = (1505 - 825\ X)\ \dot{w}$$

where X = percent ammonia dissociation, and

$$(19)\quad \dot{Q}_1 = \dot{Q}_2 + \dot{Q}_3 + \dot{Q}_L$$

Also

$$(20)\quad \dot{Q}_2 = U_2 A_2\ (T_w - T_s)$$

$$(21)\quad \dot{Q}_3 = h_1 A_3\ (T_w - T_g)$$

$$(22)\quad \dot{Q}_4 = h_2 A_4\ (T_s - T_g)$$

where $\dot{Q}_o$ = net heat generated chemically, BTU/sec

$\dot{Q}_1$ = electrical heat input, BTU/sec

$\dot{Q}_2$ = heat flux from wall to screen pack, BTU/sec

$\dot{Q}_3$ = heat flux from wall to gas, BTU/sec

$\dot{Q}_L$ = heat losses from wall, BTU/sec (defined by Figure 2-5)

$\dot{Q}_4$ = heat flux from screen to gas, BTU/sec

and U_2 = wall conductivity, $BTU/in^2 °R\ sec$

A_2 = effective screen pack/wall contact area, in^2

T_w, T_s = wall and screen pack bulk temperature, °R

h_1 = film heat transfer coefficient between wall and gas, $BTU/in^2 °R\ sec$

h_2 = film heat transfer coefficient between screen pack and gas, $BTU/in^2 °R\ sec$

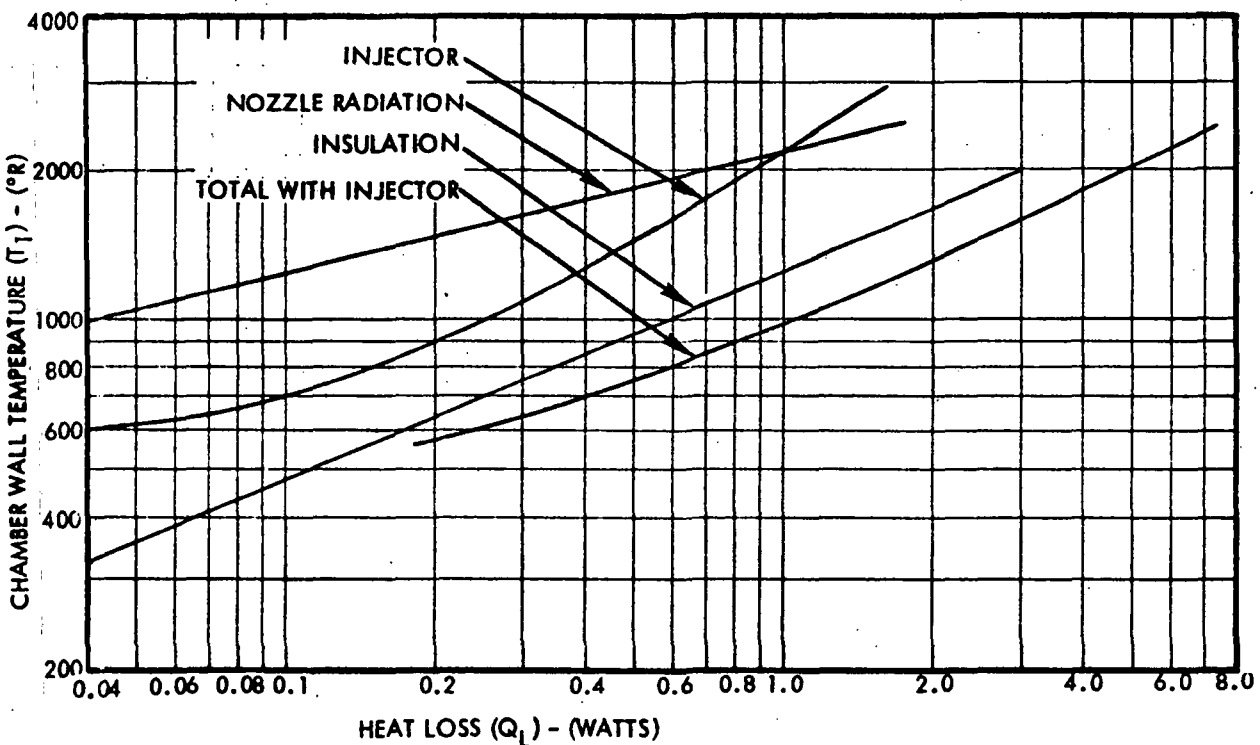

Figure 2-5 PREDICTED THERMAL LOSS VERSUS THRUSTER WALL TEMPERATURE

A_3 = effective heat transfer area between wall and gas, in^2

A_4 = effective heat transfer area between screen pack and gas, in^2

T_g = gas bulk temperature in screen pack, °R

Net heat gained by the gas in the chamber (ΔT) is defined by

$$(23) \quad \dot{w}_3 C_p \Delta T = \sum \dot{Q} = \dot{Q}_o + \dot{Q}_3 + \dot{Q}_4$$

and

$$(24) \quad T_c = T_2 + \Delta T$$

where T_2, temperature in head-end is assumed to be vapor temperature for existing chamber pressure conditions (see Figure 2-6)

Thrust is defined by

$$(25) \quad F = P_c A_t C_f$$

and steady-state specific impulse (I_{sp}) by

$$(26) \quad I_{sp} = \frac{F}{\dot{w}}$$

In the above equations, empirical relationships derived from Reference 1 and Reference 3 were used to establish C_p. Film heat transfer coefficient values were assumed to be defined approximately by the Bartz equation (Reference 3) for nozzle throat conditions where

$$(27) \quad h = \left[\frac{0.026}{D_t^{\,2}} \left(\frac{\mu^{0.2} C_p}{P_r^{0.6}} \right) \left(\frac{P_c g}{C^*} \right)^{0.8} \left(\frac{D_t}{R_c} \right)^{0.1} \right] \text{BTU/sec°R in}^2$$

and D_t = diameter at throat, in

μ = viscosity, lb/in-sec

P_r = Prandtl number

R_c = throat radius of curvature, in

C_p = gas specific heat

Also,

$$(28) \quad C^* = \frac{(g\gamma RT)^{1/2}}{\gamma^{1/2} \left(\left(\frac{2}{\gamma+1} \right)^{\frac{\gamma+1}{\gamma-1}} \right)^{1/2}}$$

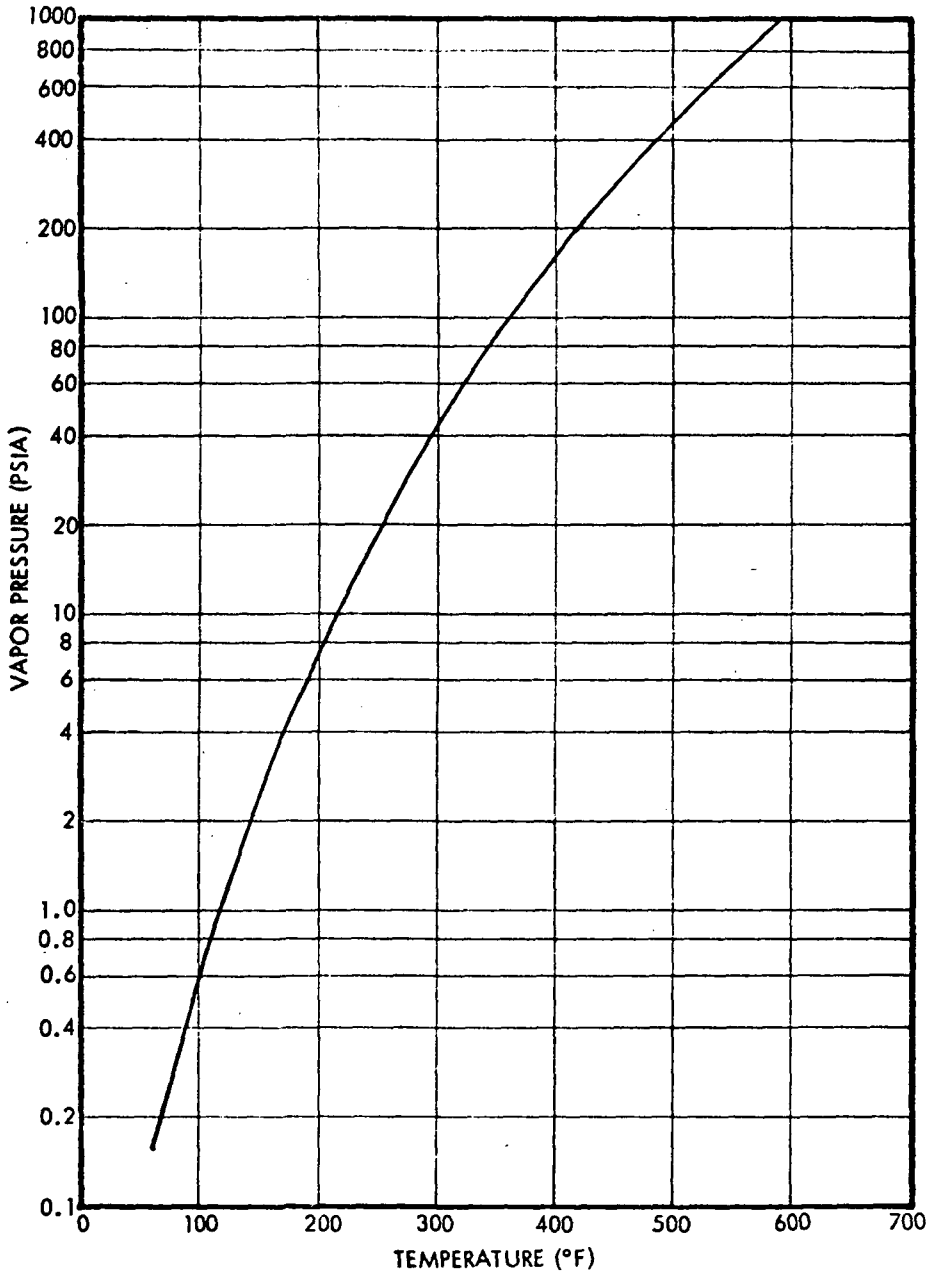

Figure 2-6 HYDRAZINE VAPOR PRESSURE

The program includes a subroutine to calculate the ideal C_f directly based on the gas properties and nozzle expansion ratio; from Reference 4,

$$(29)\quad C_{F_T} = \left[\left(\frac{2\gamma^2}{\gamma-1}\right)\left(\frac{2}{\gamma+1}\right)^{\frac{\gamma+1}{\gamma-1}}\left(1-\left(\frac{P_e}{P_c}\right)^{\frac{\gamma-1}{\gamma}}\right)\right]^{1/2} + \frac{P_e}{P_c}\varepsilon - \frac{P_a}{P_c}\varepsilon$$

where γ = gas specific heat ratio

C_{F_T} = theoretical thrust coefficient

P_e = nozzle exit pressure, psi

P_a = ambient pressure (assumed = 0)

ε = nozzle expansion ratio

and where

$$(30)\quad \varepsilon = \frac{\left(\frac{2}{\gamma+1}\right)^{\frac{\gamma+1}{2(\gamma-1)}}}{\left(\frac{P_e}{P_c}\right)^{\frac{1}{\gamma}}\left[\frac{2}{\gamma-1}\left(1-\left(\frac{P_e}{P_c}\right)^{\frac{\gamma-1}{\gamma}}\right)\right]^{1/2}}$$

actual C_f is defined by,

$$(31)\quad C_f = C_{F_T}\ \eta$$

where

η = efficiency factor (defined emperically $\approx .87$).

2.4 Transient Analysis

2.4.1 Introduction

The thruster transient computer model was formulated on a C15000 active element analog computer. The analog is particularly amenable to this type of study, since the engineering equations can be simulated in a modular form. This facilitates changing the model to include different configurational or operational conditions. The analog program provides time variant analog data such as would be obtained from actual hardware testing. This is particularly useful in evaluating test data since performance parameters not measurable in testing (flowrate, etc) are produced as direct analytical outputs.

In operation, program inputs include: specified thruster dimensions (injector area, head-end and chamber volume, etc), supply pressure and temperature, and nozzle thrust coefficient. Values for specific heat, specific heat ratio and gas constant, are included tabularly as a function of dissociation fraction which is also currently specified as an input. Calculated parameters include thruster flow rates, thrust, chamber and internal pressures, screen pack, wall and gas bulk temperatures, impulse and specific impulse. The computer schematic is shown in Figure 2-7, and the analytical model is summarized in Section 2.4.2.

2.4.2 Analytical Model

As with the steady-state model, the transient thruster model is based on lumped parameter considerations whereby mass, resistance, and temperature are represented by single lumped nodes. The mathematical model is derived from conservation of mass and energy relationships as follows: (Nomenclature is identical to that defined in Section 2.3.2 for the Steady-State Analytical Model).

Flow through the valve is defined by

$$(32)\quad \dot{w}_1 = C_D A_v \left[\rho 2g\ (P_o - P_1)\right]^{1/2}$$

and injector inlet pressure by

$$(33)\quad \frac{dP_1}{dt} = \frac{\beta}{\rho AL}\ (\dot{w}_1 - \dot{w}_2)$$

where β = propellant bulk modulus, lb/in^2, L = tube length, inch, and injector flow and head-end pressure are defined by

$$(34)\quad \dot{w}_2 = C_D A_i \left[\rho 2g\ (P_1 - P_2)\right]^{1/2}$$

and

$$(35)\quad \frac{dP_2}{dt} = \frac{\gamma R T_2}{V_2}\ (\dot{w}_2 - \dot{w}_3)$$

Temperature in the head-end is assumed defined by a vapor pressure/temperature relationship such that

$$(36)\quad T_2 = f(P_2)\quad \text{[See Figure 2-5]}$$

Screen pack flow is given by

$$(37)\quad \dot{w}_3 = K_1 \left[\frac{P_3}{RT_3}(P_2 - P_c)\right]^{1/2}$$

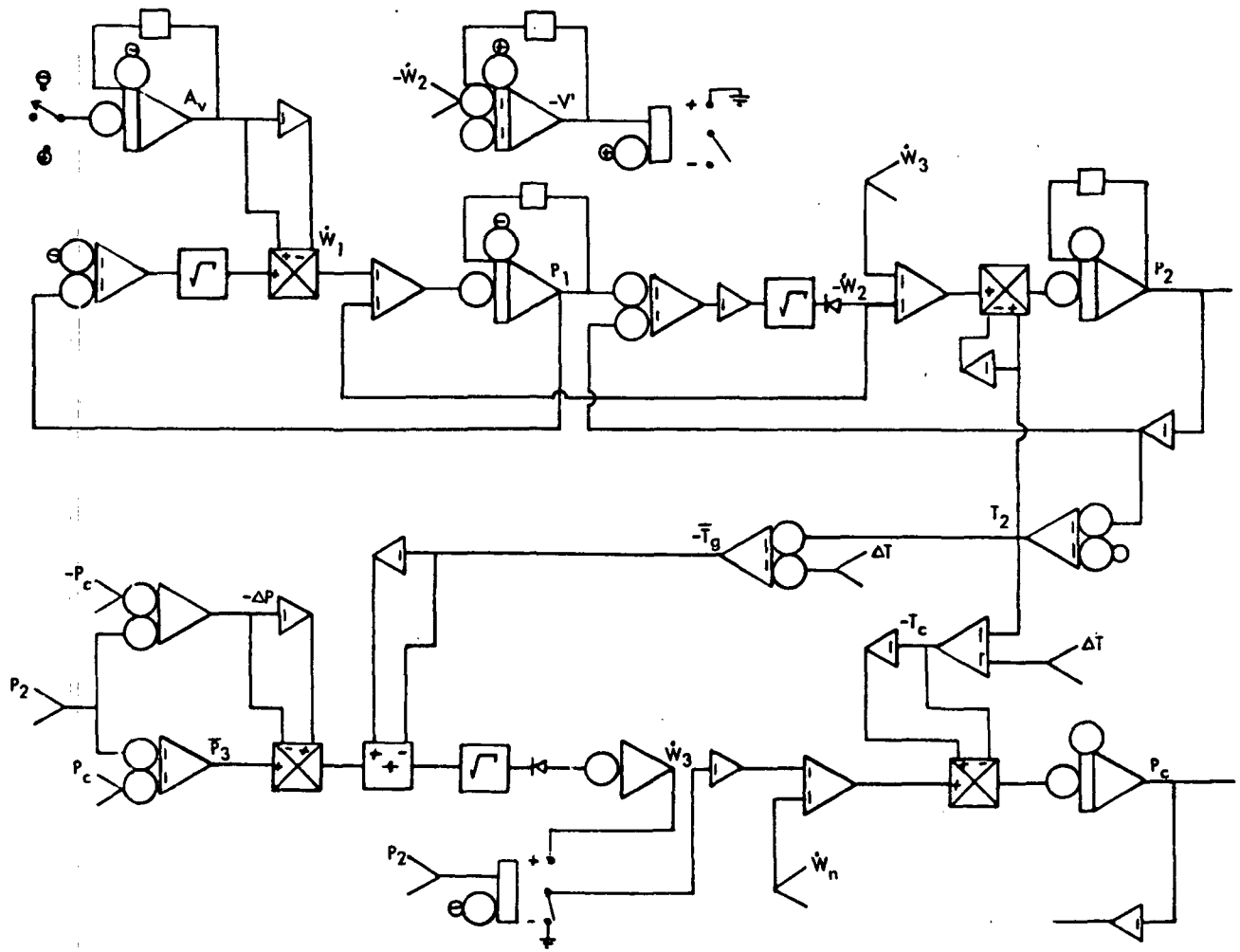

Figure 2-7a ELECTROTHERMAL HYDRAZINE THRUSTER ANALOG COMPUTER MODEL SCHEMATIC

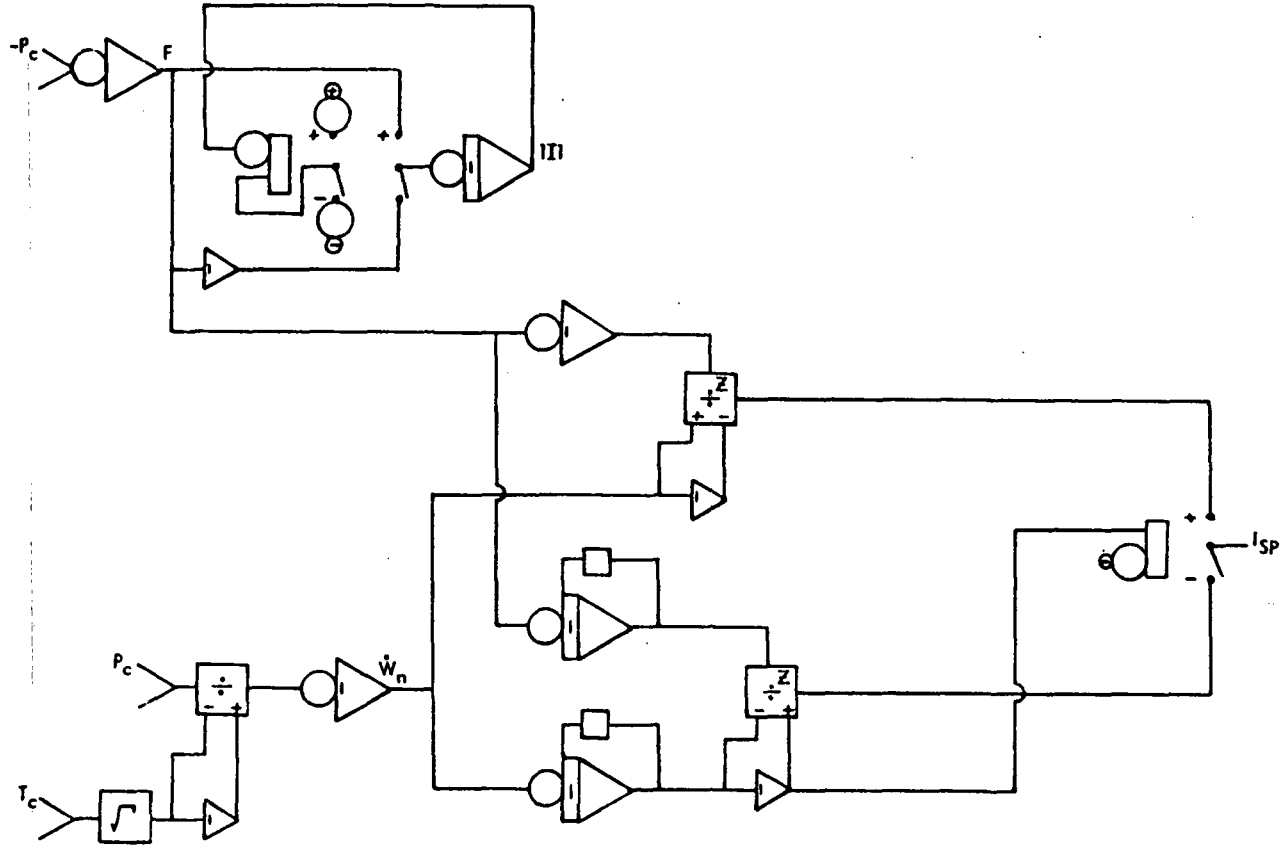

Figure 2-7b ELECTROTHERMAL HYDRAZINE THRUSTER ANALOG COMPUTER MODEL SCHEMATIC

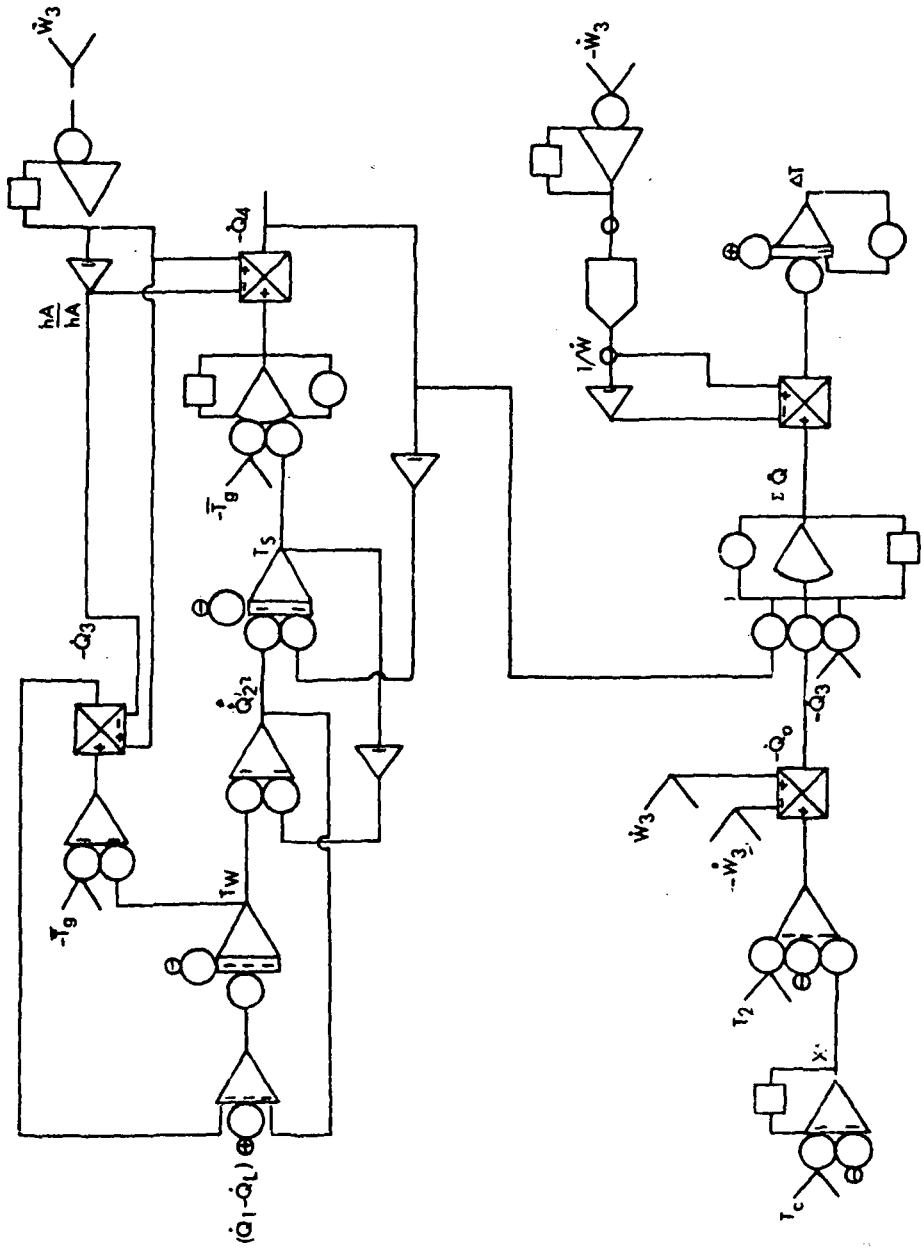

Figure 2-7c ELECTROTHERMAL HYDRAZINE THRUSTER ANALOG COMPUTER MODEL SCHEMATIC

where P_3, average screen pack pressure, is

$$(38)\quad P_3 = \frac{P_2 + P_c}{2}$$

T_3, Average gas temperature in the screen (T_3), is given by

$$(39)\quad T_3 = T_2 + \frac{1}{2}\ \Delta T$$

where ΔT, temperature increase of gas in the chamber, is defined by Equation 23. Chamber pressure and nozzle flow are defined by

$$(40)\quad \frac{dP_c}{dt} = \frac{\gamma R T_g}{V_c}\ (\dot{w}_3 - \dot{w}_n)$$

and nozzle flowrate is established by

$$(41)\quad \dot{w}_n = \frac{P_c A_t g}{C^*}$$

where

$$(42)\quad C^* = \frac{(g\gamma RT)^{1/2}}{\gamma\left[\left(\frac{2}{\gamma+1}\right)^{\frac{\gamma+1}{\gamma-1}}\right]^{1/2}}$$

The chemical heat input is characterized by

$$(43)\quad \dot{Q}_o = [1505 - 825\ X]\ \dot{w}_3$$

with wall temperature defined by

$$(44)\quad \frac{dT_w}{dt} = (C_w M_w)^{-1}\ [\dot{Q}_1 - \dot{Q}_2 - \dot{Q}_3 - \dot{Q}_L]$$

Heat flux from wall to screen pack is given by

$$(45)\quad \dot{Q}_2 = UA_2\ (T_w - T_s)$$

and screen pack temperature by

$$(46)\quad \frac{dT_s}{dt} = (C_s M_s)^{-1}\ [\dot{Q}_2 - \dot{Q}_4]$$

C_w and C_s are the chamber wall and screen pack specific heat.
M_w and M_s represent the mass of the wall and screen pack, respectively, and heat flux from wall to gas is defined by

$$(47)\quad \dot{Q}_3 = hA_3\ (T_w - T_g)$$

Heat flux from screen pack to gas is

$$(48)\quad \dot{Q}_4 = hA_4\ (T_s - T_g)$$

Net temperature gain by the gas is

$$(49)\quad \dot{w}_3 C_p \Delta T = \dot{Q}_o + \dot{Q}_3 + \dot{Q}_4$$

and chamber gas temperature

$$(50)\quad T_g = T_2 + \Delta T \quad \text{(where } T_g = T_c = \text{gas bulk temperature in screen pack)}$$

Priming logic in the model is such that $\dot{w}_2 = 0$ until time = t_p where

$$(51)\quad V_p = \frac{1}{\rho} \int_o^{t_p} \dot{w}_1 \, dt$$

and V_p (priming volume) nominal was assumed to be $5.7(10^{-4})$ in^3. Also, thrust and specific impulse are established by

$$(52)\quad F = P_c A_t C_f$$

$$(53)\quad I_{sp} = \frac{\int F}{\int \dot{w}}$$

3.0 COMPUTER STUDIES

3.1 Introduction

The primary intent of the studies summarized here was to provide preliminary definition of the performance range and parameter sensitivity of the Electrothermal Hydrazine Thruster. For these studies .040 lbf thrust was used as the reference point about which to evaluate the thruster performance. Unless otherwise noted, operating conditions for the data tabulated were: electrical power = 12 watts, supply pressure = 200 psi, and ambient pressure = 0 psi.

3.2 Steady-State Studies

3.2.1 Summary

Evaluation of steady-state operation included consideration of the effects of supply pressure, thermal losses and electrical power on thruster performance. The effects of these parameters on steady-state thrust, specific impulse, and characteristic velocity are summarized in the following sections.

3.2.2 Supply Pressure and Electrical Power

The variation in steady-state thrust with supply pressure and electrical power is shown in Figure 3-1. The effects of blowdown operation on thrust are evident since thrust decreases nearly linearly with supply pressure, from .040 lbf at 200 psi to .025 lbf at 100 psi.

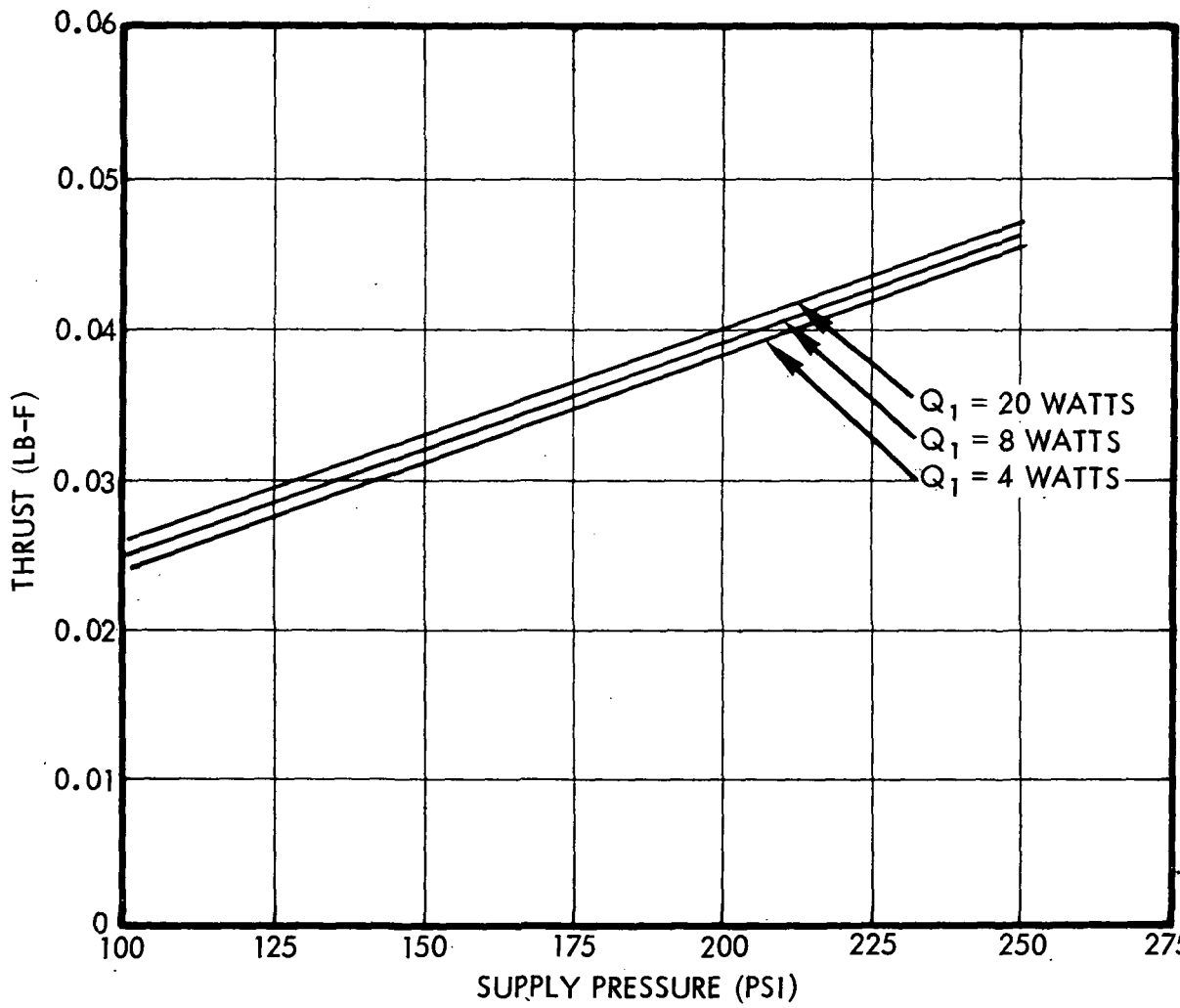

Figure 3-1 STEADY STATE THRUST VERSUS SUPPLY PRESSURE AND ELECTRICAL POWER

Variations in electrical power from 4 to 20 watts have only a small effect on thrust and, as shown in the computer printout of Figure 3-2, a fairly large electrical input is required to noticeably increase thrust. The effects on specific impulse of supply pressure and electrical power are crossplotted in Figures 3-3 and 3-4. Increased electrical power provides a significant gain in specific impulse and at power levels above 12 watts, specific impulse increases with decreasing supply pressure. Similarly, supply pressure variations over a blowdown range of from 200 to 100 psi result in a 1 to 2% decrease in specific impulse at low power levels (below approximately 12 watts). At higher power levels, specific impulse is increased during supply pressure blowdown. Variations in steady-state characteristic velocity with supply pressure and electrical power are summarized in Figure 3-5. Similar to specific impulse, the characteristic velocity over a blowdown range of from 250 to 100 psi varies only slightly at power levels below 12 watts. At higher power levels, characteristic velocity increases with decreasing supply pressure. (Theoretically the characteristic velocity is 4865 ft/sec at 100 psi and 60 watts and 4676 ft/sec at 250 psi and 60 watts.)

3.2.3 Dissociation Fraction

Ammonia dissociation fraction was specified as an input and not calculated as a program output. Computer runs were made to evaluate the effects of specified variations in percent ammonia dissociation, as shown in Figures 3-6 through 3-8. Dissociation fraction (which influences gas constant, specific heat ratio, and net chemical energy) primarily influences specific impulse and characteristic velocity. Specific impulse values of from 215 to 226 seconds and characteristic velocity values of from 4300 ft/sec to 4500 ft/sec resulted over a dissociation range of from 0.2 to 0.7. As seen in Figure 3-6, the effect on thrust is relatively small.

3.2.4 Thermal Losses

This study essentially provided an indication of the relative effect on performance of thruster thermal insulation. In the steady-state program, thermal losses are defined as a function of wall temperature. Based on this data, thermal losses during normal operation are approximately 5.4 watts. Reduction or slight increase of this value results in little change to characteristic velocity, specific impulse and thrust, since the loss values are small relative to the 230 watt chemical input (see Figures 3-9 through 3-11).

```
***INPUTS***

SUPPLY PRESSURE          =  2.000E+02  PSIA
SUPPLY TEMPERATURE       =  7.000E+01  DEGREES F
ELECTRICAL PØWER INPUT   =  1.000E+02  WATTS
DISSØCIATIØN FRACTIØN    =  3.000E-01
INJECTØR AREA            =  4.480E-06  SQUARE INCHES
THRØAT AREA              =  3.140E-04  SQUARE INCHES
EXPANSIØN RATIØ          =  5.000E+01

---ØUTPUT---

INJECTØR INLET PRESSURE       =  1.409E+02  PSIA
HEAD END PRESSURE             =  8.712E+01  PSIA
AVERAGE SCREEN PACK PRESSURE  =  8.531E+01  PSIA
CHAMBER PRESSURE              =  8.350E+01  PSIA

VAPØRIZATIØN TEMPERATURE  =  3.429E+02  DEGREES F
AVERAGE GAS TEMPERATURE   =  2.091E+03  DEGREES F
SCREEN PACK TEMPERATURE   =  2.093E+03  DEGREES F
WALL TEMPERATURE          =  2.160E+03  DEGREES F
CHAMBER TEMPERATURE       =  2.760E+03  DEGREES F

CHEMICAL HEAT INPUT       =  2.263E+02  WATTS
WALL TØ SCREEN HEAT FLUX  =  1.096E+01  WATTS
WALL TØ GAS HEAT FLUX     =  8.074E+01  WATTS
SCREEN TØ GAS HEAT FLUX   =  1.096E+01  WATTS
HEAT LØSSES               =  8.303E+00  WATTS

THRUST CØEFFICIENT  =  1.654E+00
FLØWRATE            =  1.707E-04  LBS./SEC.
THRUST              =  4.336E-02  LBS.-F
SPECIFIC IMPULSE    =  2.540E+02  SEC.
CSTAR               =  4.946E+03  FT/SEC.
```

Figure 3-2 EHT Steady State Computer Output Data - 100 Watt Electrical Power

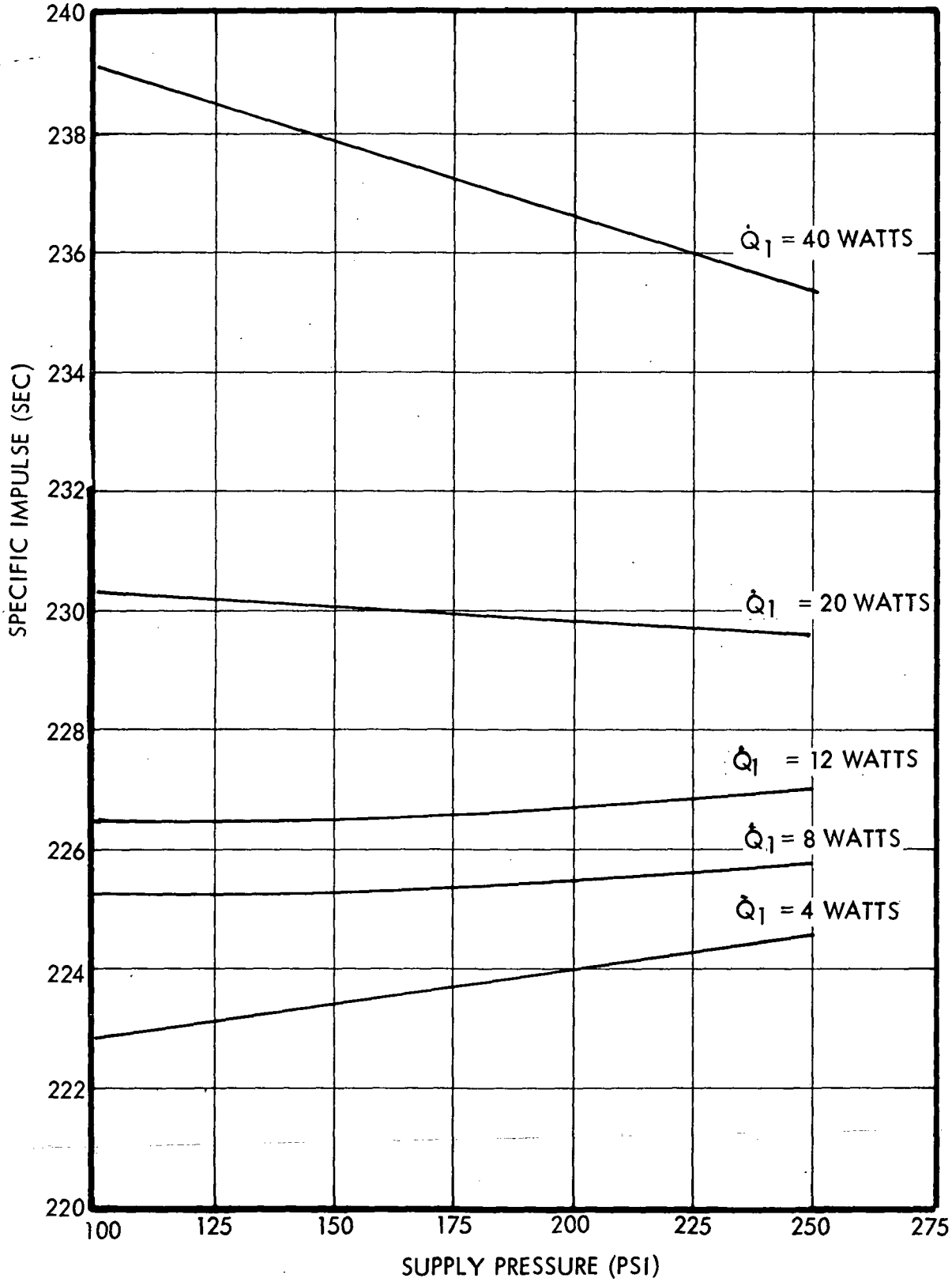

Figure 3-3 STEADY STATE SPECIFIC IMPULSE VERSUS SUPPLY PRESSURE

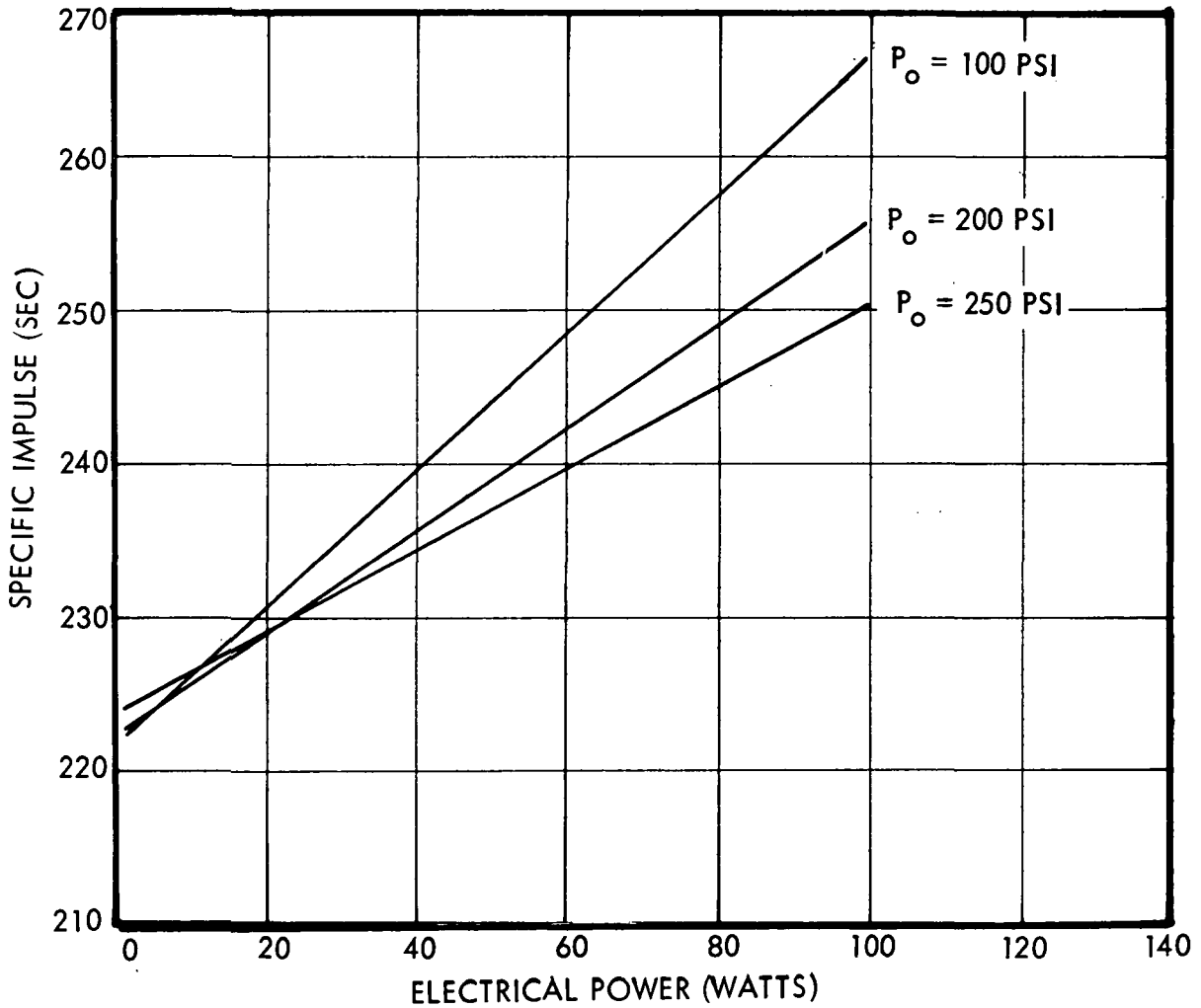

Figure 3-4 STEADY STATE SPECIFIC IMPULSE VERSUS ELECTRICAL POWER

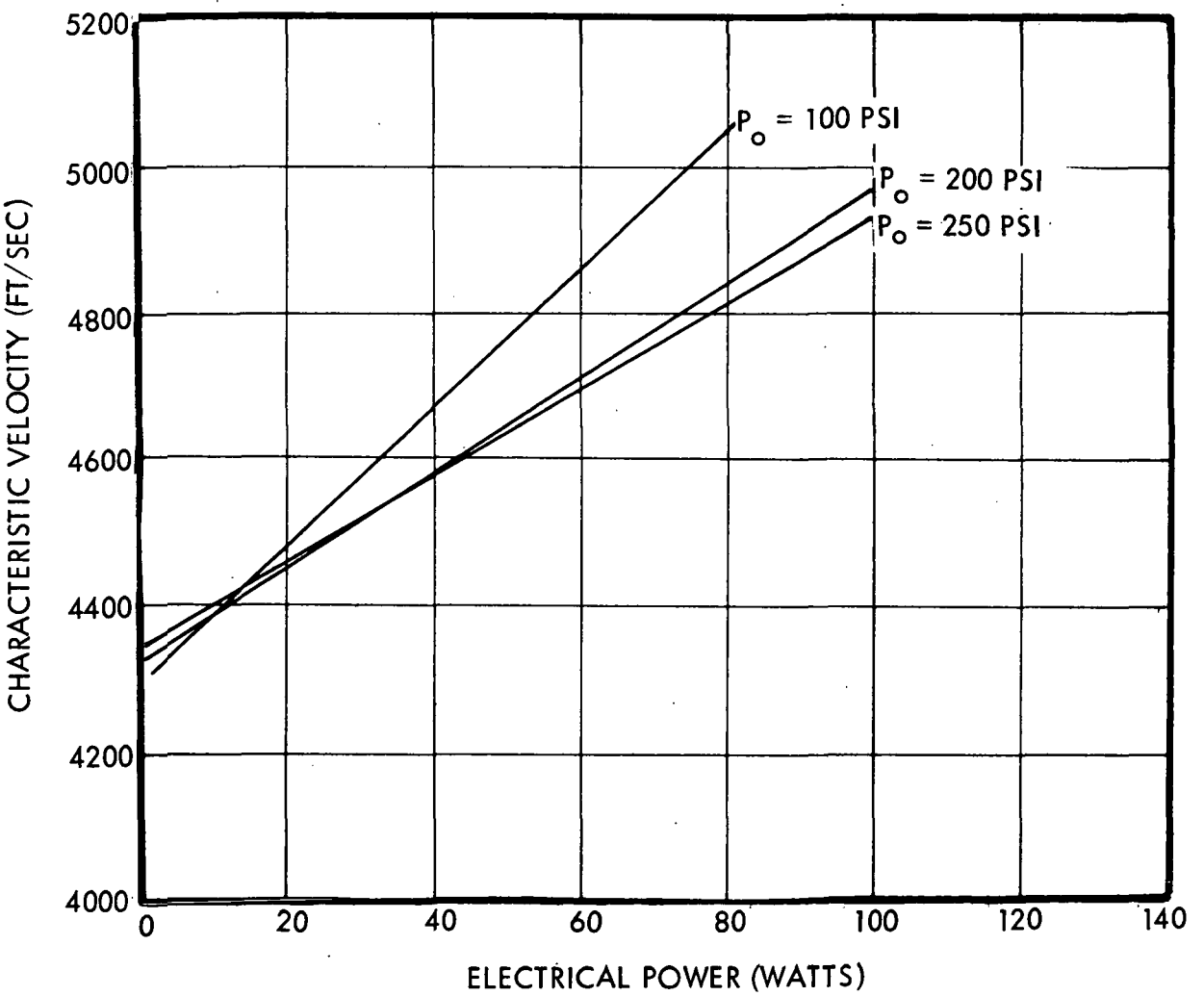

Figure 3-5 STEADY STATE CHARACTERISTIC VELOCITY VERSUS SUPPLY PRESSURE AND ELECTRICAL POWER

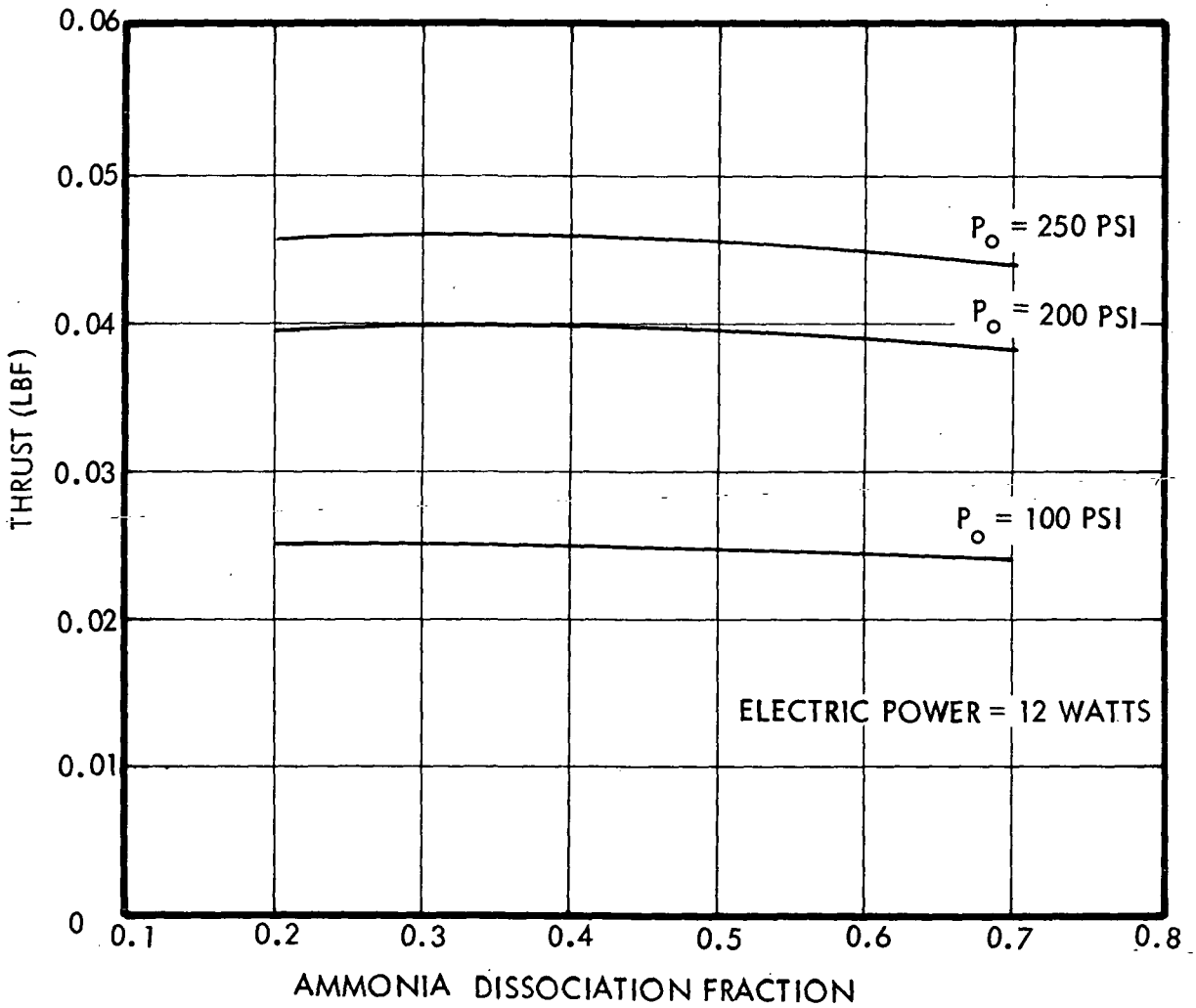

Figure 3-6 STEADY STATE THRUST VERSUS AMMONIA DISSOCIATION FRACTION AND SUPPLY PRESSURE

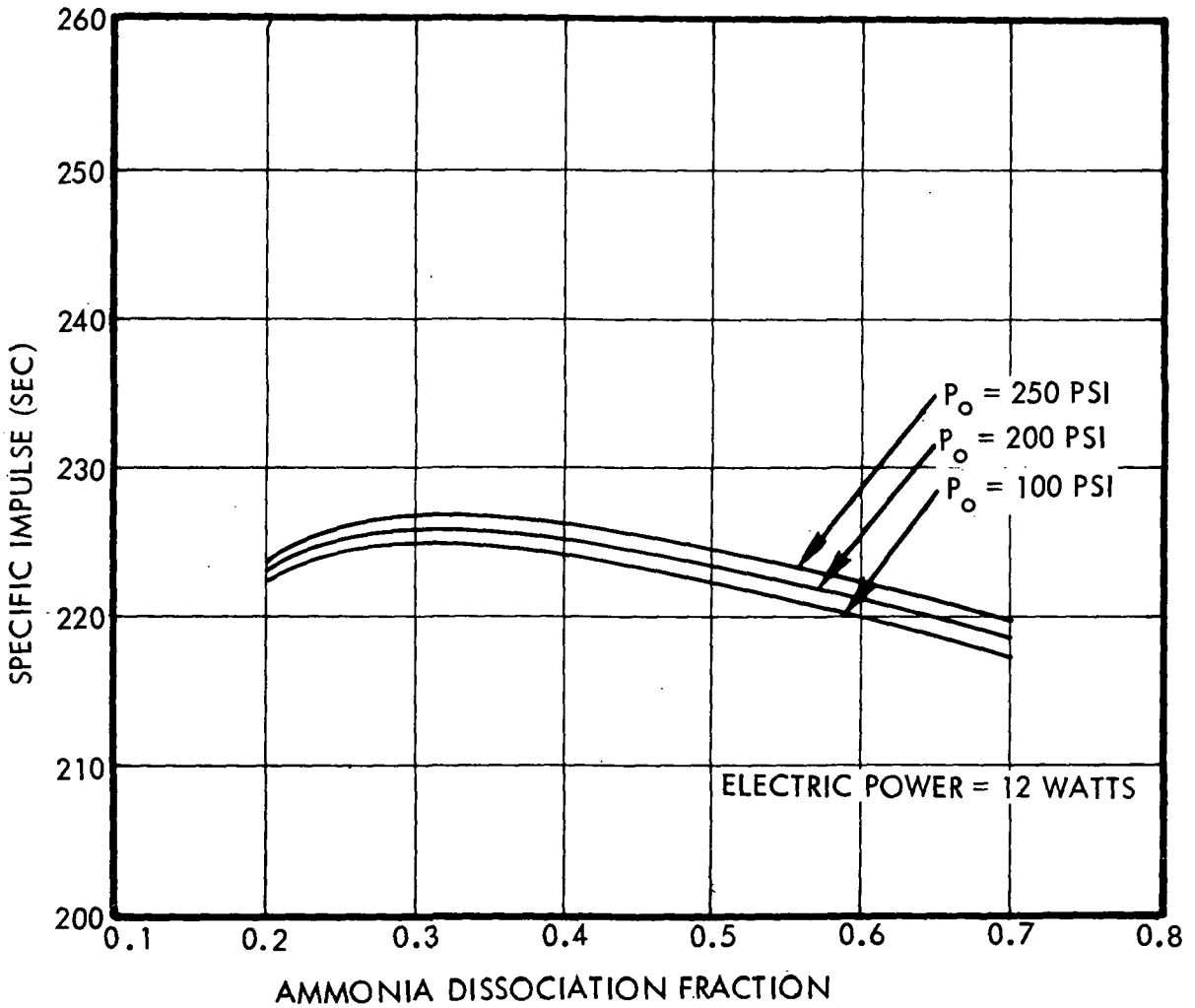

Figure 3-7 STEADY STATE SPECIFIC IMPULSE VERSUS AMMONIA DISSOCIATION FRACTION AND SUPPLY PRESSURE

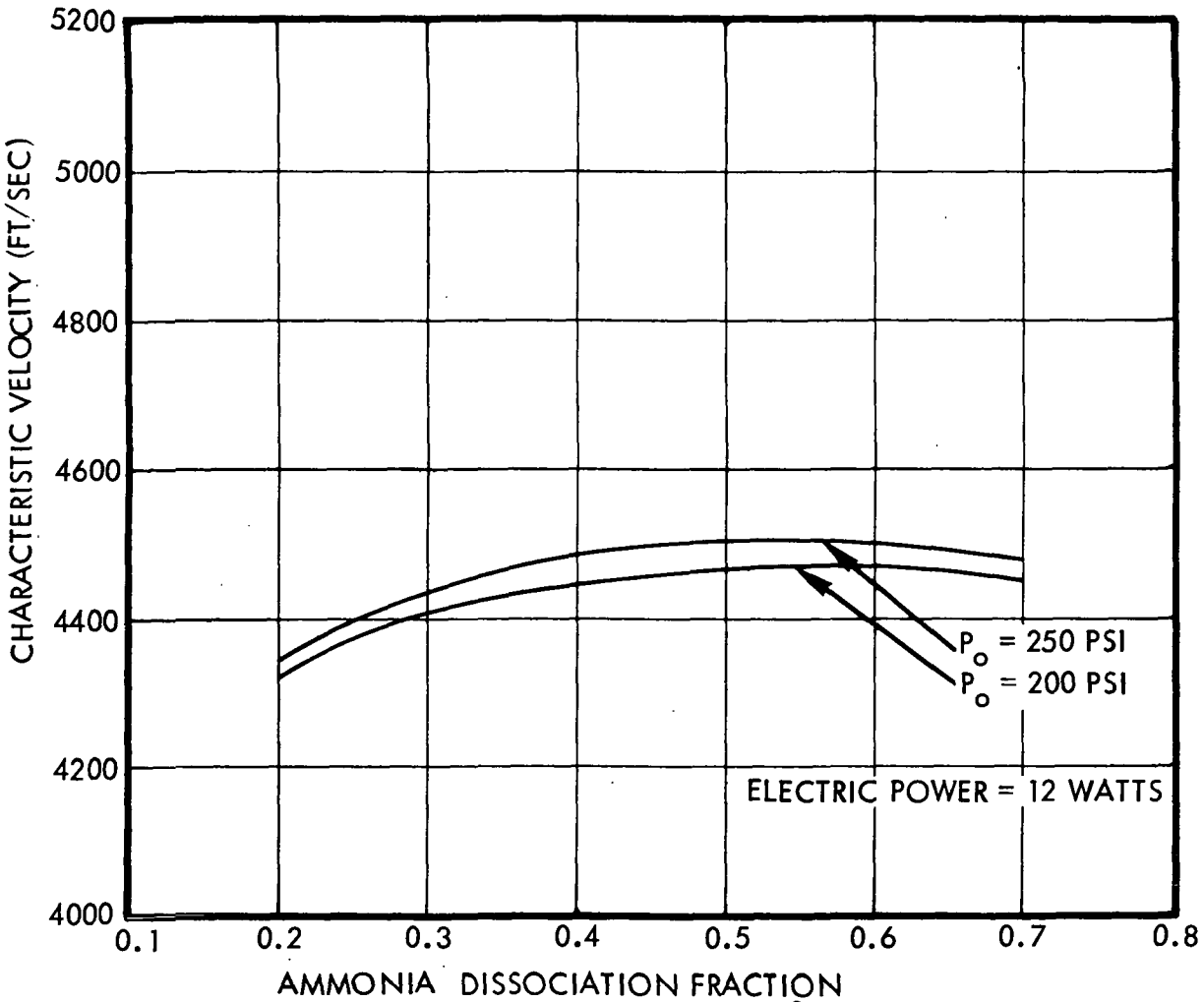

Figure 3-8 STEADY STATE CHARACTERISTIC VELOCITY VERSUS AMMONIA DISSOCIATION FRACTION AND SUPPLY PRESSURE

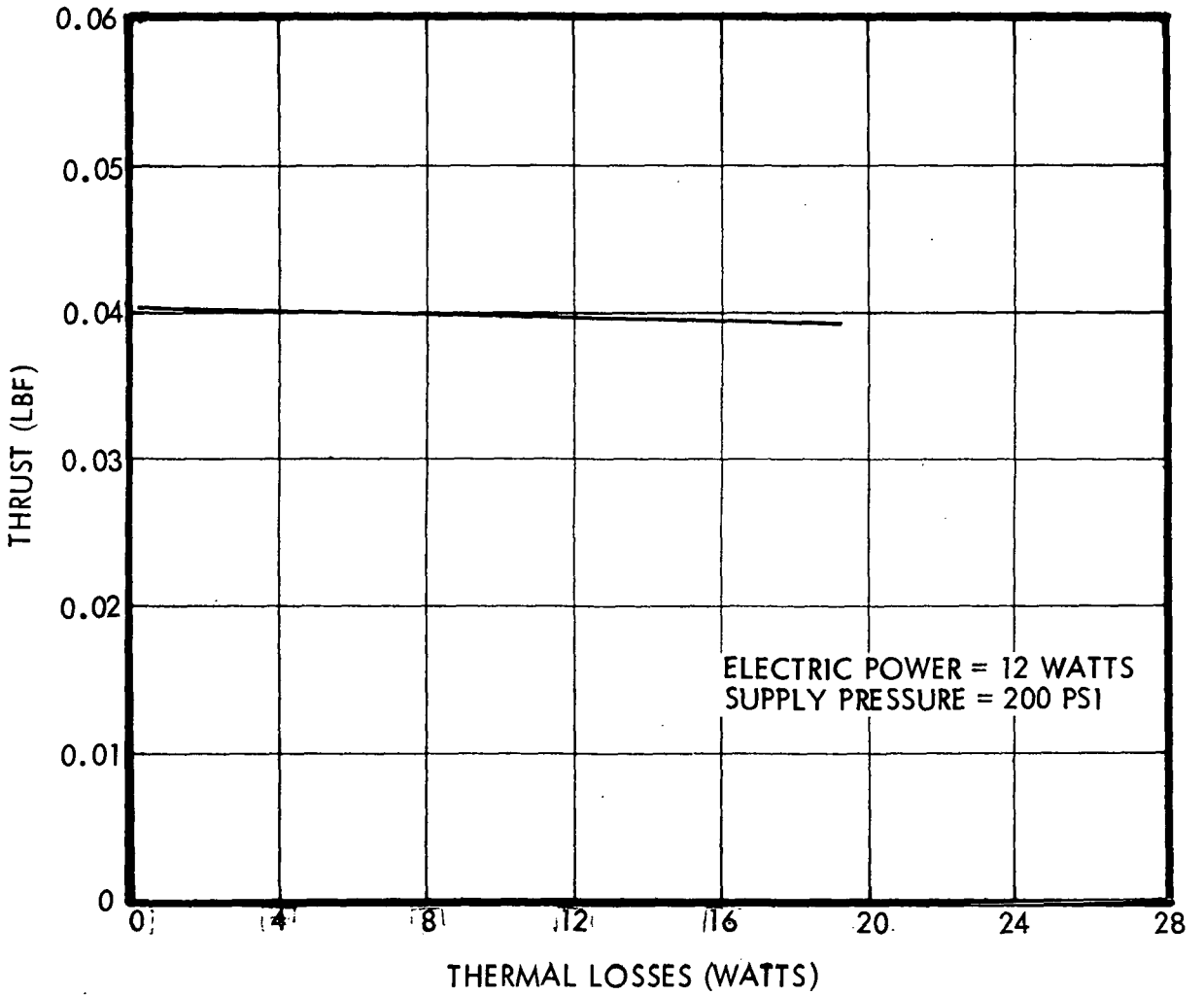

Figure 3-9 STEADY STATE THRUST VERSUS THERMAL LOSSES

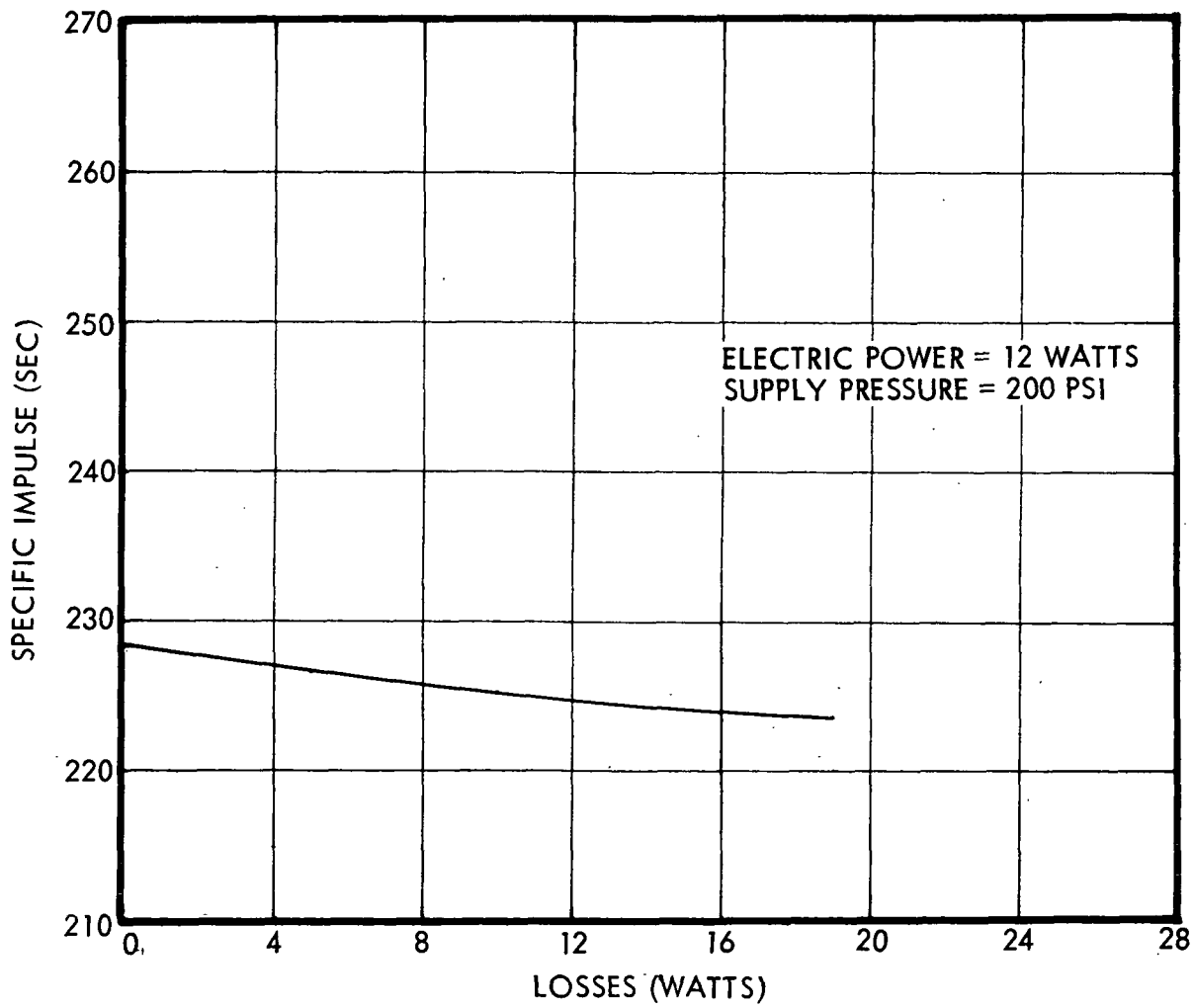

Figure 3-10 STEADY STATE SPECIFIC IMPULSE VERSUS THERMAL LOSSES

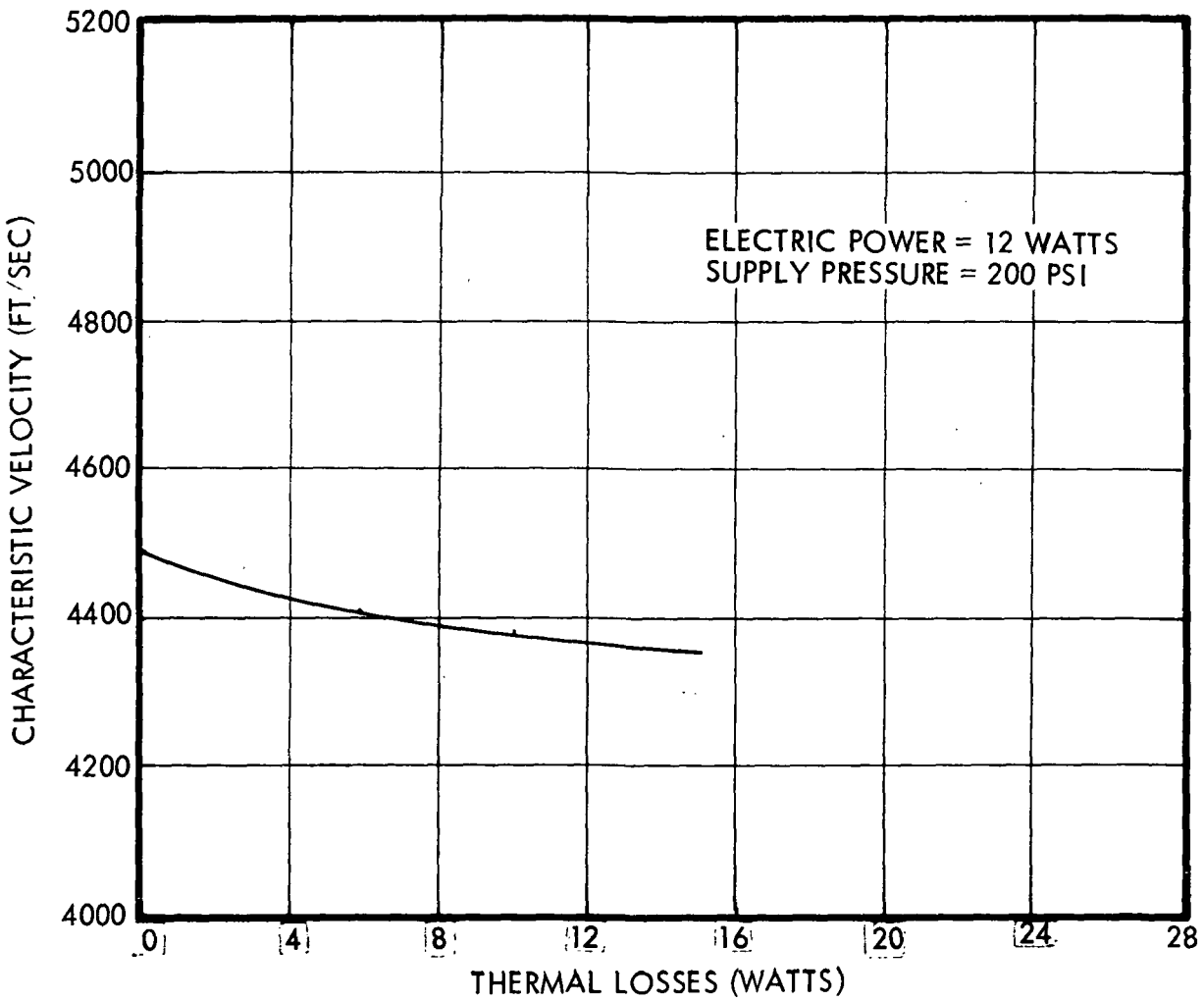

Figure 3-11 STEADY STATE CHARACTERISTIC VELOCITY VERSUS THERMAL LOSSES

3.2.5 Design Parameter Effects

An evaluation was made of steady-state performance sensitivity to design factors such as chamber wall and screen pack areas, head end volume, chamber volume, and injector and throat areas. Since the models do not currently represent detailed gas kinetics, volume and area have negligible effect on steady-state operation. The model is not currently sophisticated enough to evaluate such effects as head end/injector entrance angle or impingement of liquid on the screen pack face. The influence on thrust and specific impulse of injector flow area (Figure 3-12) shows little variation. Much of the inlet-to-chamber pressure drop occurs in the thruster solenoid valve.

3.3 Transient Studies

3.3.1 Summary

Studies with the transient computer model included consideration of duty cycle, operational, and design configuration effects. Duty cycle effects include consideration of 25,50 and 100 millisecond pulses, as well as long burns from the holding conditions to steady-state.

Studies includedevaluation of the effects of holding temperature, electrical power and supply pressure, as well as design parameters such as thruster weight, chamber wall area and screen pack area. (Typical pulse mode and steady-state start-up computer data is shown in Figure 3-13A and 3-13B). Note that pulse operation is characterized by rapid rise and tail-off of the chamber pressure, thrust, and internal pressures. Flowrate is primarily regulated by valve and injector area (valve response is about 2 milliseconds) and a slight overshoot in flowrate results at start due to the absence of chamber back pressure.

Startup to steady-state is characterized by a rapid rise to the pulse mode specific impulse, thrust and gas temperature (Note that the startup shown is from a holding temperature of 1000°R), followed by a gradual transient-rise to steady-state as the wall heats up. The sensitivity of these characteristics to the various operational and design factors are discussed in the following sections. Parameters evaluated in the following sections include impulse bit, specific impulse, time to reach steady-state from start, and number of pulses versus specific impulse for pulsed duty cycle with constant pulse widths.

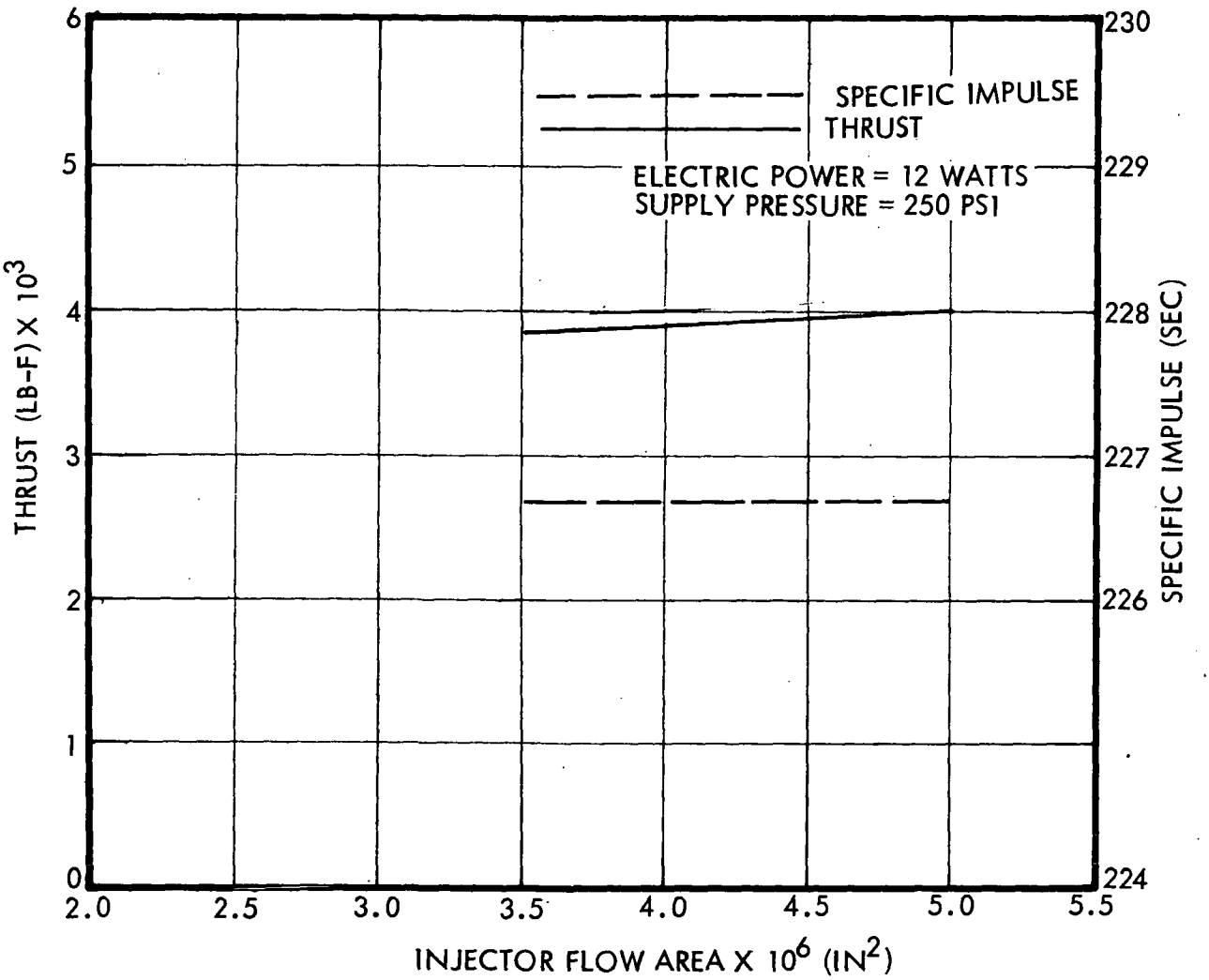

Figure 3-12 STEADY STATE THRUST AND SPECIFIC IMPULSE VERSUS INJECTOR FLOW AREA

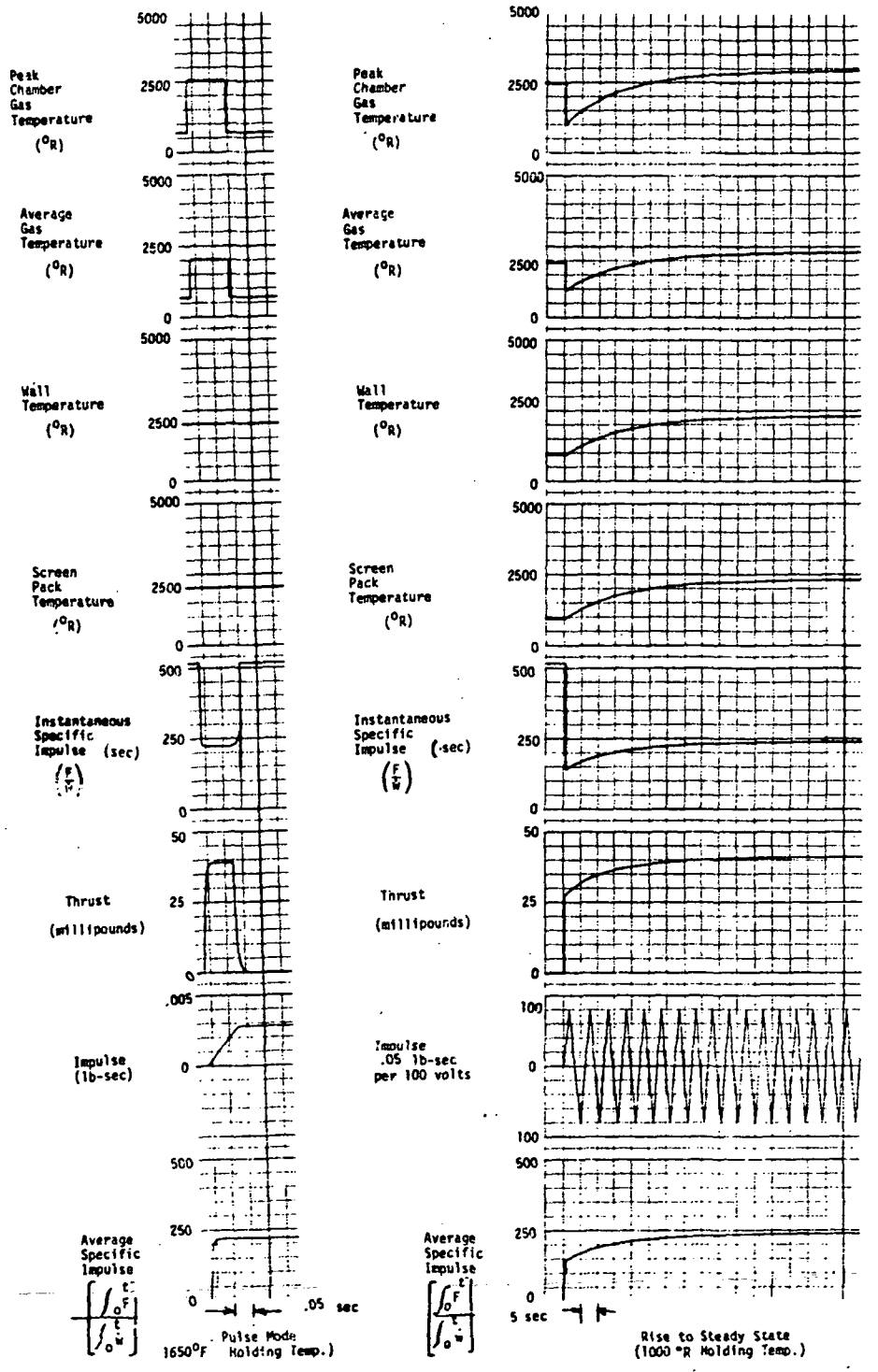

Figure 3-13a TYPICAL TRANSIENT PERFORMANCE DATA FROM ANALOG MODEL (SUPPLY PRESSURE = 200 PSI)

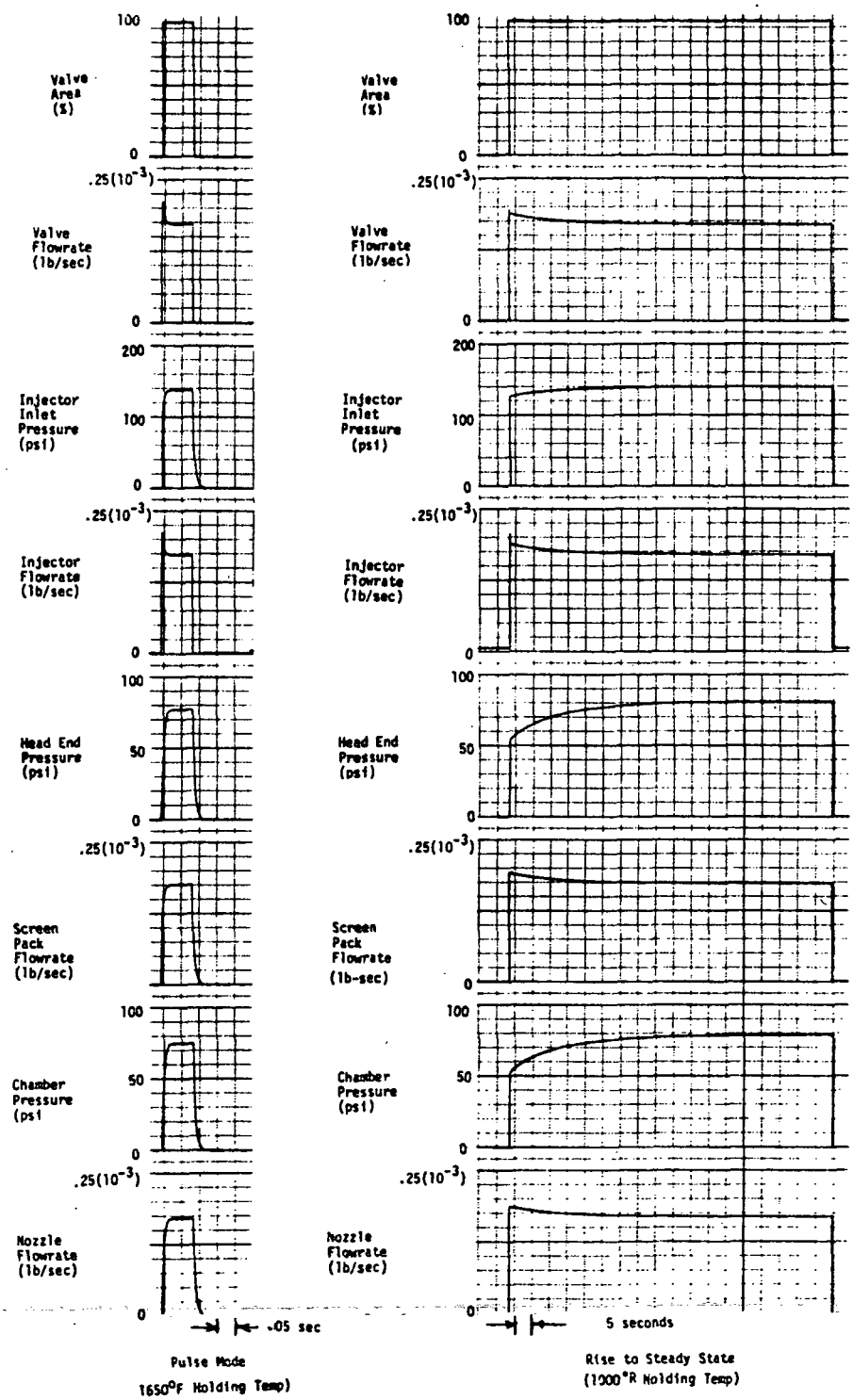

Figure 3-13b TYPICAL TRANSIENT PERFORMANCE DATA FROM ANALOG MODEL (SUPPLY PRESSURE = 200 PSI)

3.3.2 Supply Pressure and Holding Temperature

The effects of supply pressure and holding temperature on transient and pulse mode operation are summarized in Figures 3-14 through 3-17. As illustrated in Figures 3-14a and 3-14b, supply pressure has only a small effect on rise time to steady-state with only a 5 second increase in time for a 150 psi drop in supply pressure (from 250 to 100 psi). As indicated by this data, the change in rise time to steady-state was minimal even though the resulting steady-state thrust is strongly affected by supply pressure. Holding temperature prior to ignition has more noticeable effect, and an increase of from 500 to 1600°F would reduce rise time to steady-state to a few milliseconds, since this is the nominal operating temperature. Initial wall temperatures above 1600°F then result in a cooldown transient time to steady-state conditions (Figure 3-14b). Figures 3-15 and 3-16 show that net increases in either supply pressure or holding temperature result in increased impulse bit for pulse mode operation. Studies of specific impulse variability indicated negligible sensitivity to supply pressure. Variation in holding temperature, however, results in large variations in specific impulse as seen in Figure 3-17. The computer data in Figures 3-18 and 3-19 illustrate the proportional effects of varied holding temperature and supply pressure on pulsed operation.

Pulse mode specific impulse was found to be relatively constant for 25, 50 and 100 millisecond pulses. The predicted pulse mode specific impulse versus number of pulses and holding temperature is summarized in Figure 3-20a. As expected, the number of pulses required to reach hot thrust specific impulse values increases with decreasing pulse width. Figure 3-20b illustrates the pulse mode impulse bit versus pulse number. Similar to specific impulse, the number of pulses required to reach hot thrust impulse bit values increases with decreasing pulse width.

3.3.3 Thruster Weight Study

Studies indicated that variations in thruster weight have little effect on pulse performance, primarily affecting the rise time to steady-state

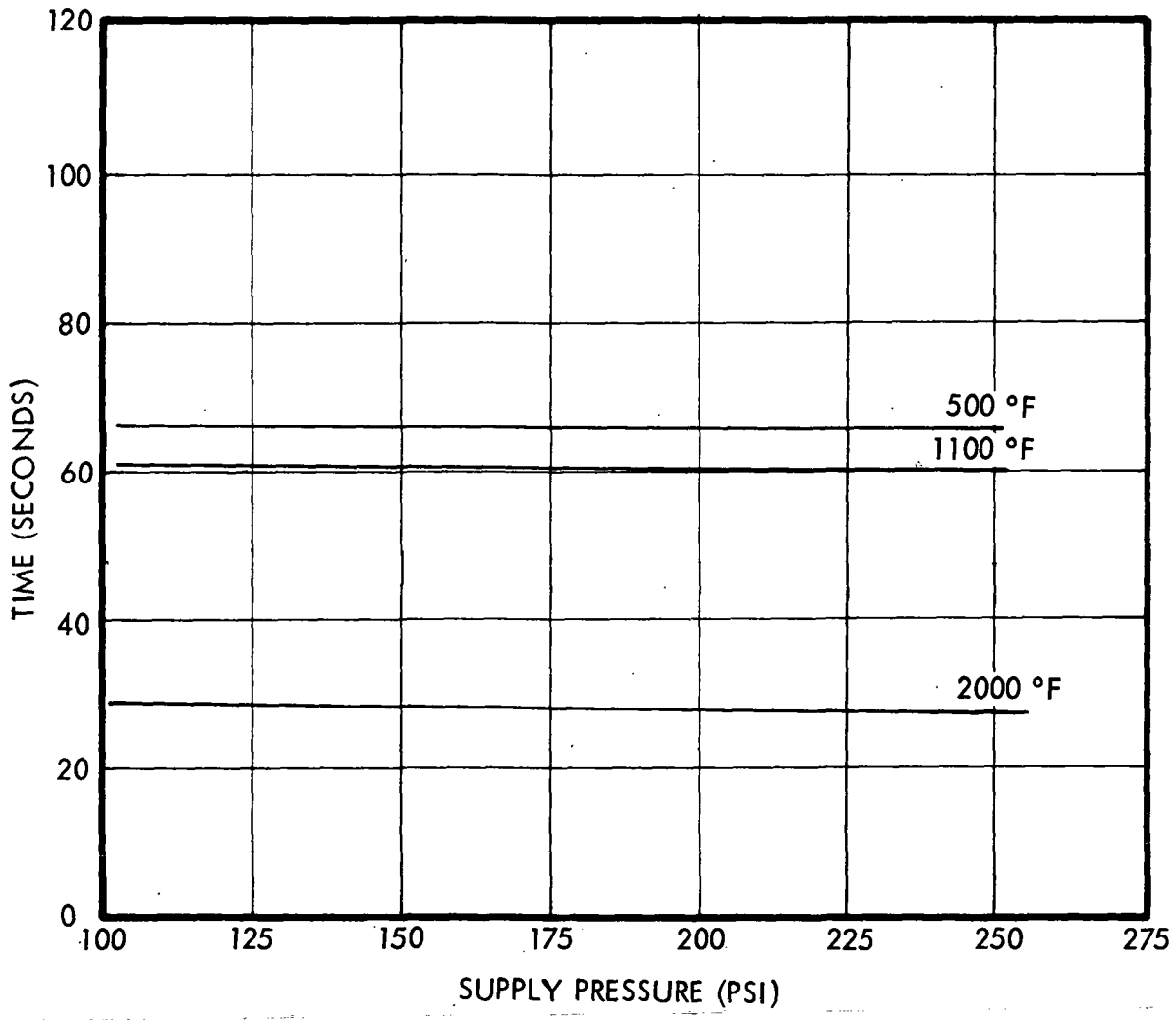

Figure 3-14a. STARTUP RISE TIME REQUIRED TO REACH STEADY STATE CONDITIONS VERSUS SUPPLY PRESSURE AND INITIAL HOLDING TEMPERATURE

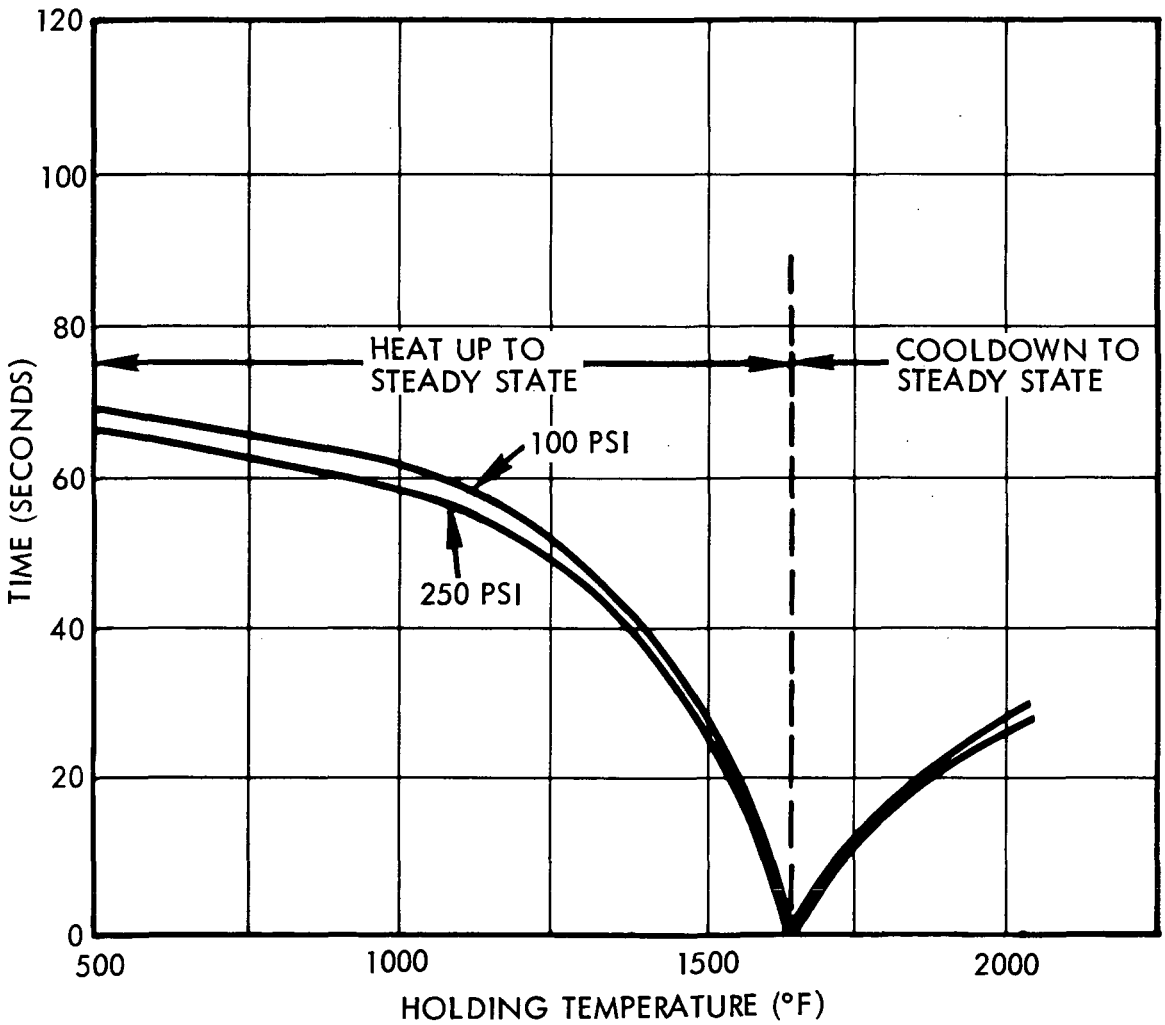

Figure 3-14b. STARTUP RISE TIME REQUIRED TO REACH STEADY STATE CONDITIONS VERSUS INITIAL HOLDING TEMPERATURE AND SUPPLY PRESSURE

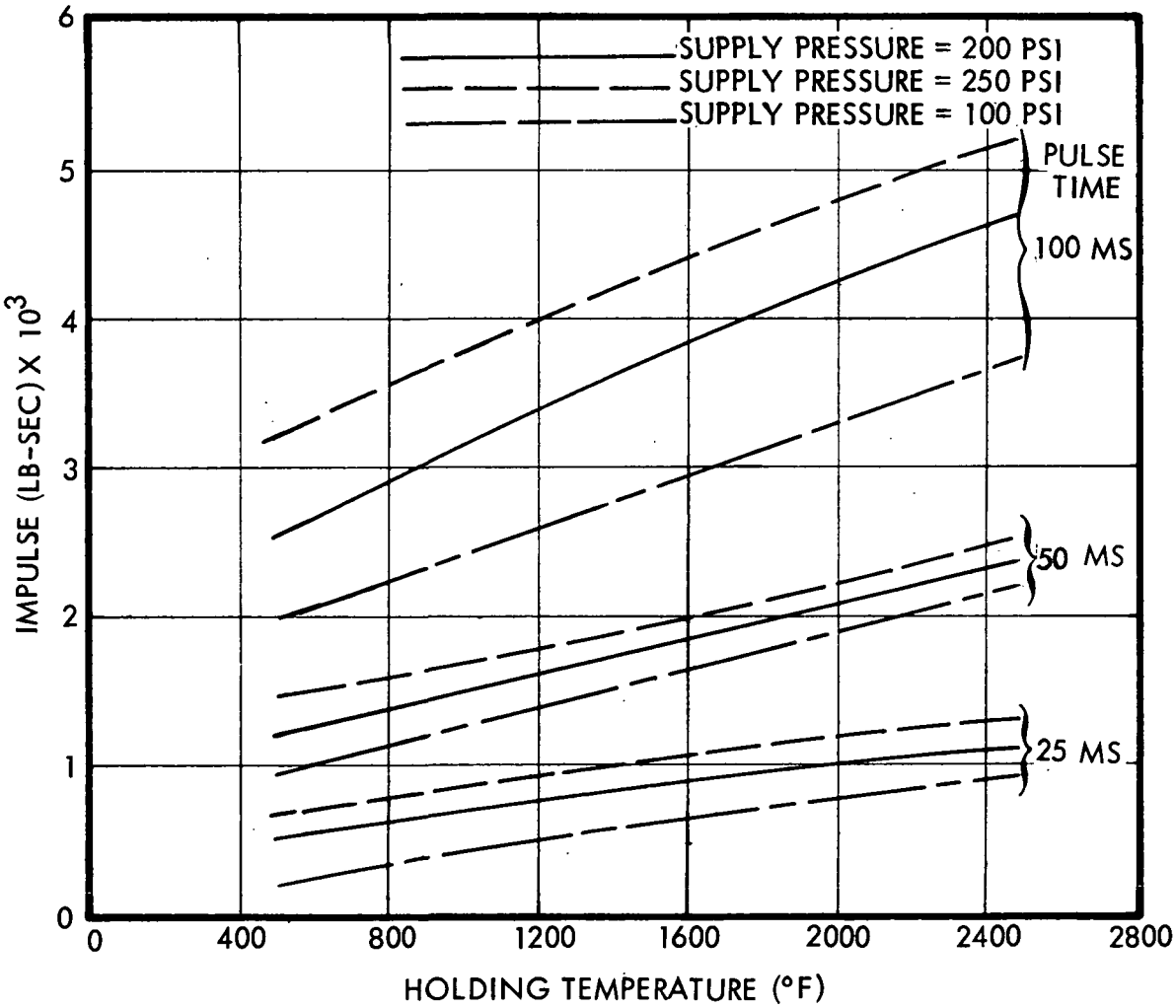

Figure 3-15 PULSE MODE IMPULSE BIT VERSUS WALL TEMPERATURE AND SUPPLY PRESSURE

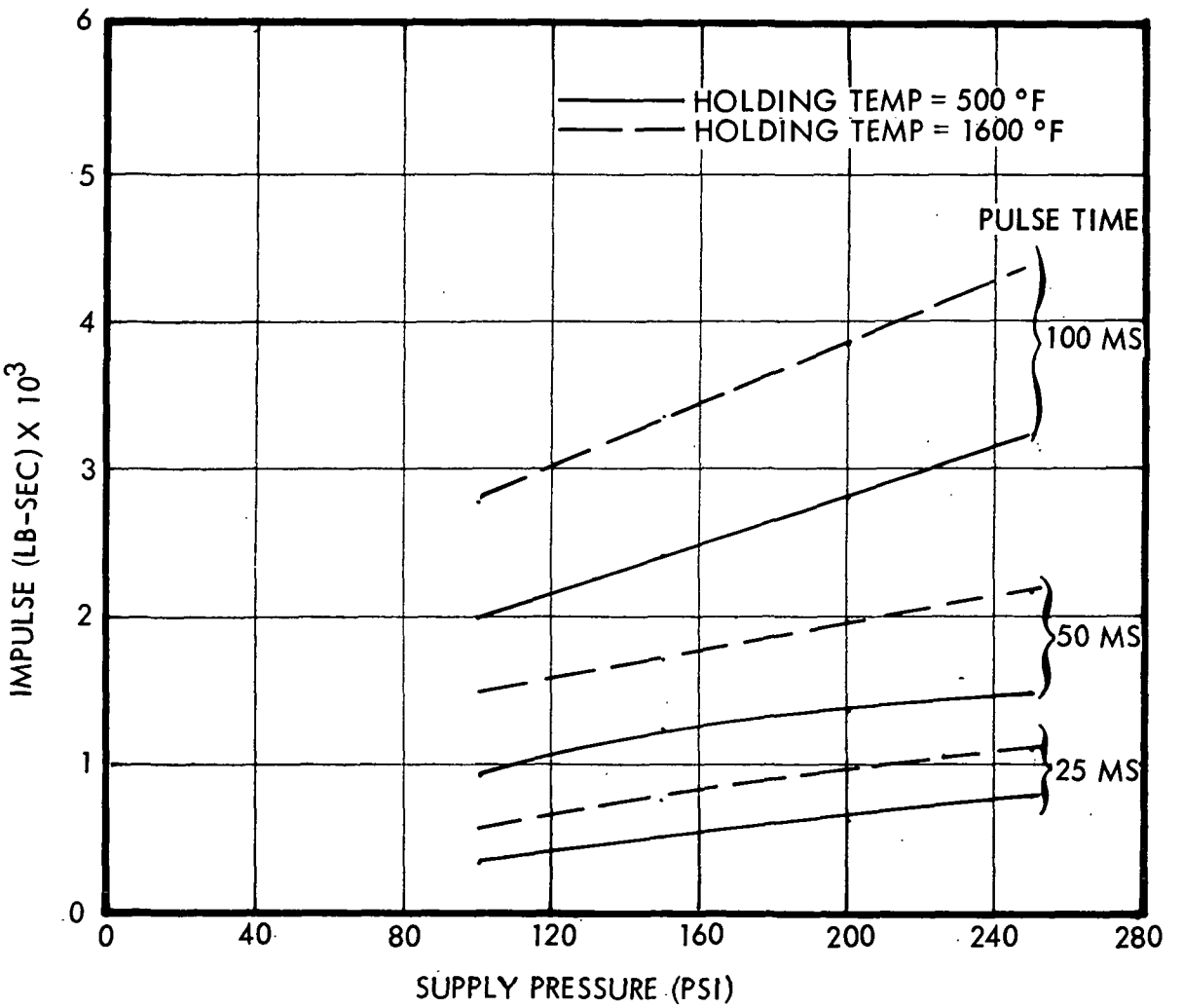

Figure 3-16 PULSE MODE IMPULSE BIT VERSUS SUPPLY PRESSURE AND WALL TEMPERATURE

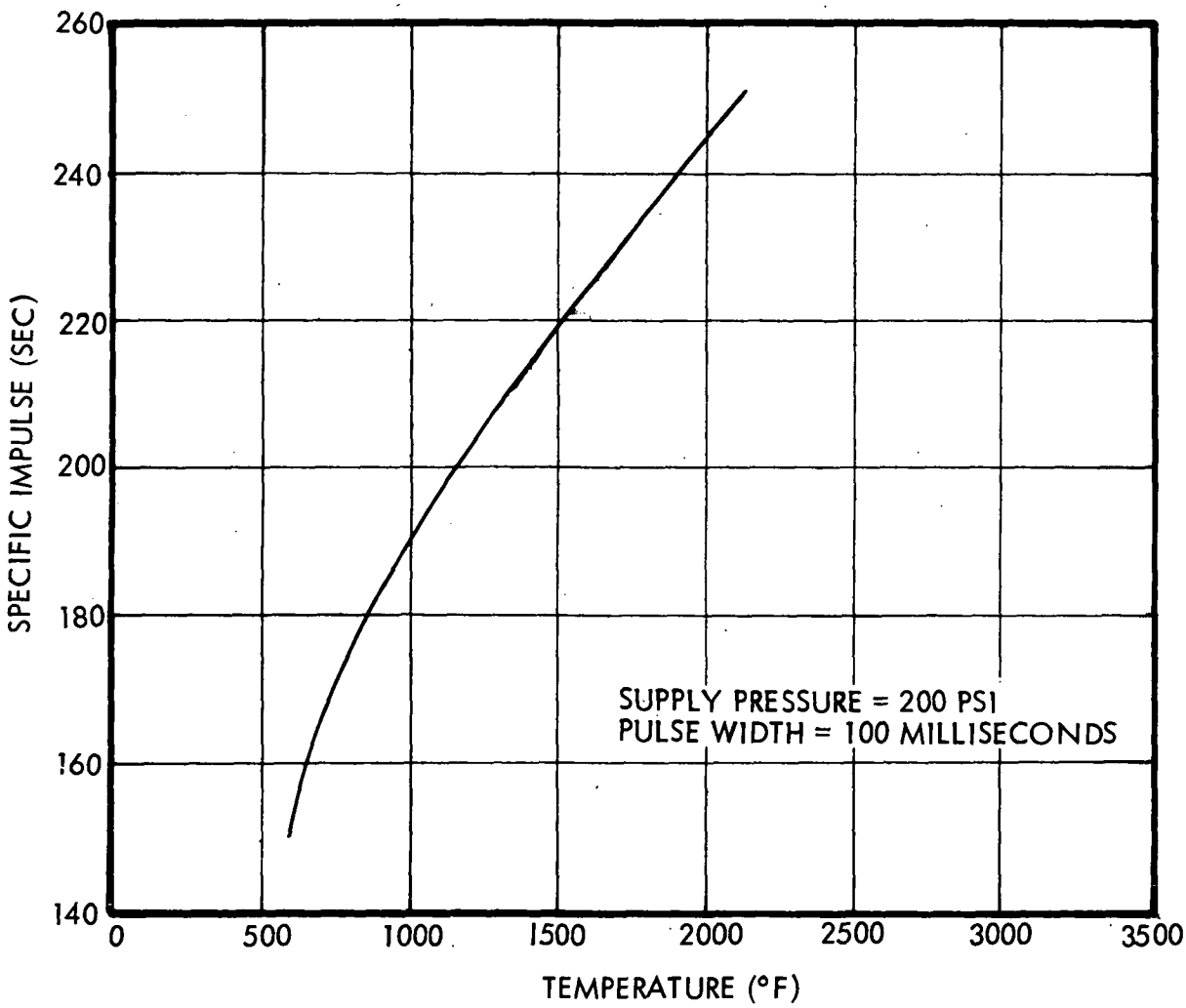

Figure 3-17 PULSE MODE SPECIFIC IMPULSE VERSUS WALL TEMPERATURE

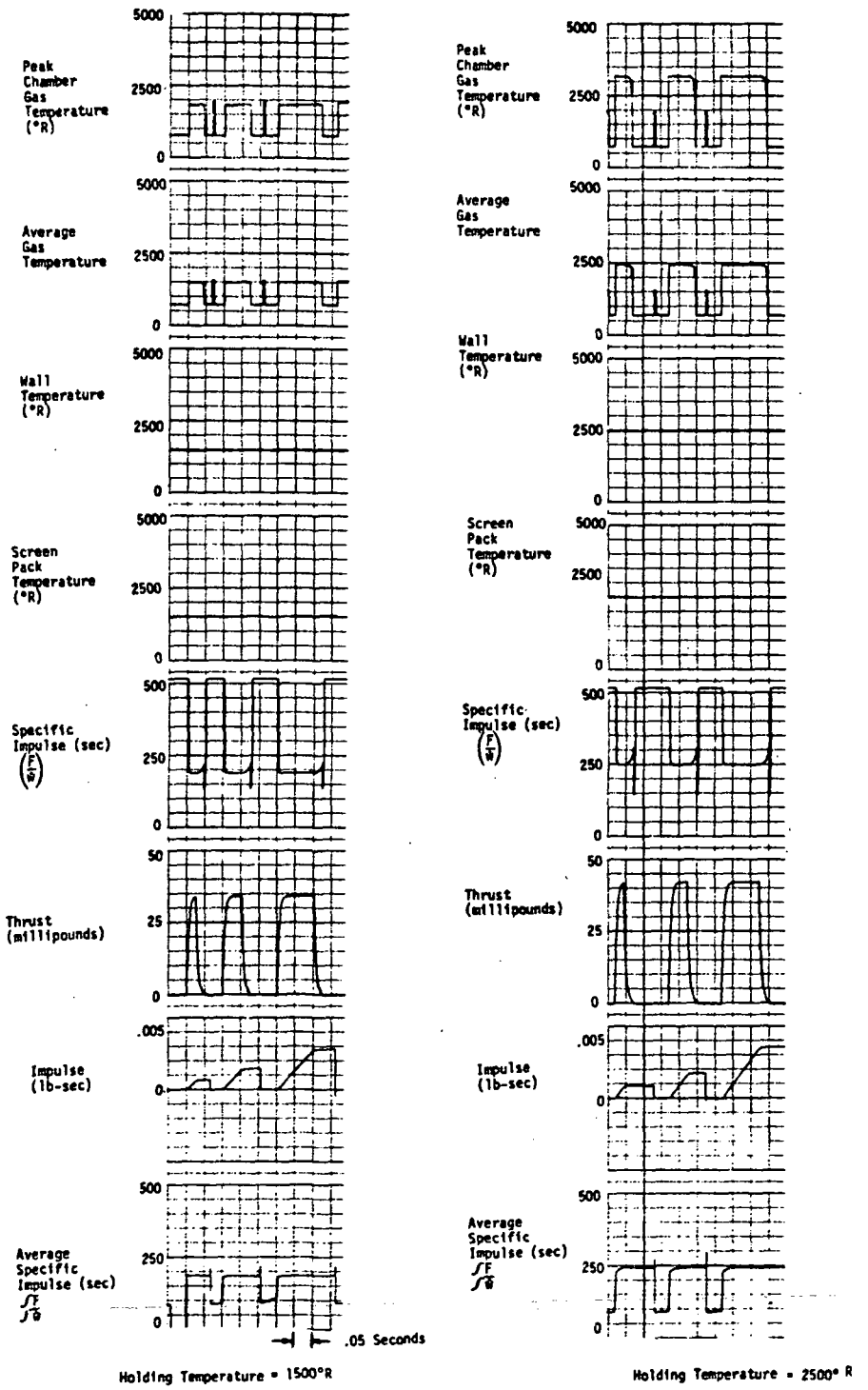

Figure 3-18 ANALOG COMPUTER TRANSIENT PERFORMANCE DATA -- WALL TEMPERATURE STUDY (SUPPLY PRESSURE = 200 PSI)

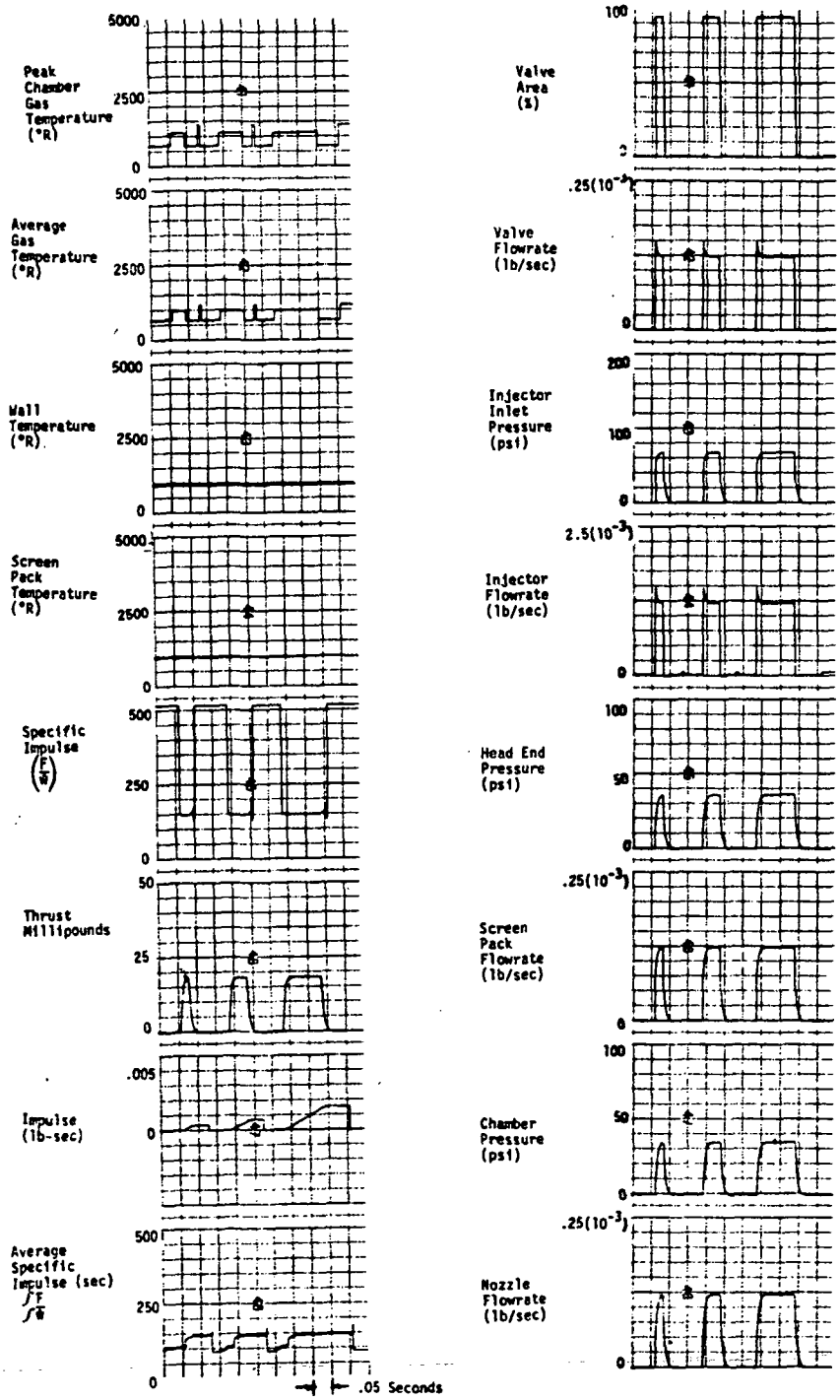

FIGURE 3-19 ANALOG COMPUTER TRANSIENT PERFORMANCE DATA -- SUPPLY PRESSURE PRESSURE STUDY (SUPPLY PRESSURE = 100 PSI, HOLDING TEMP = 500°F)

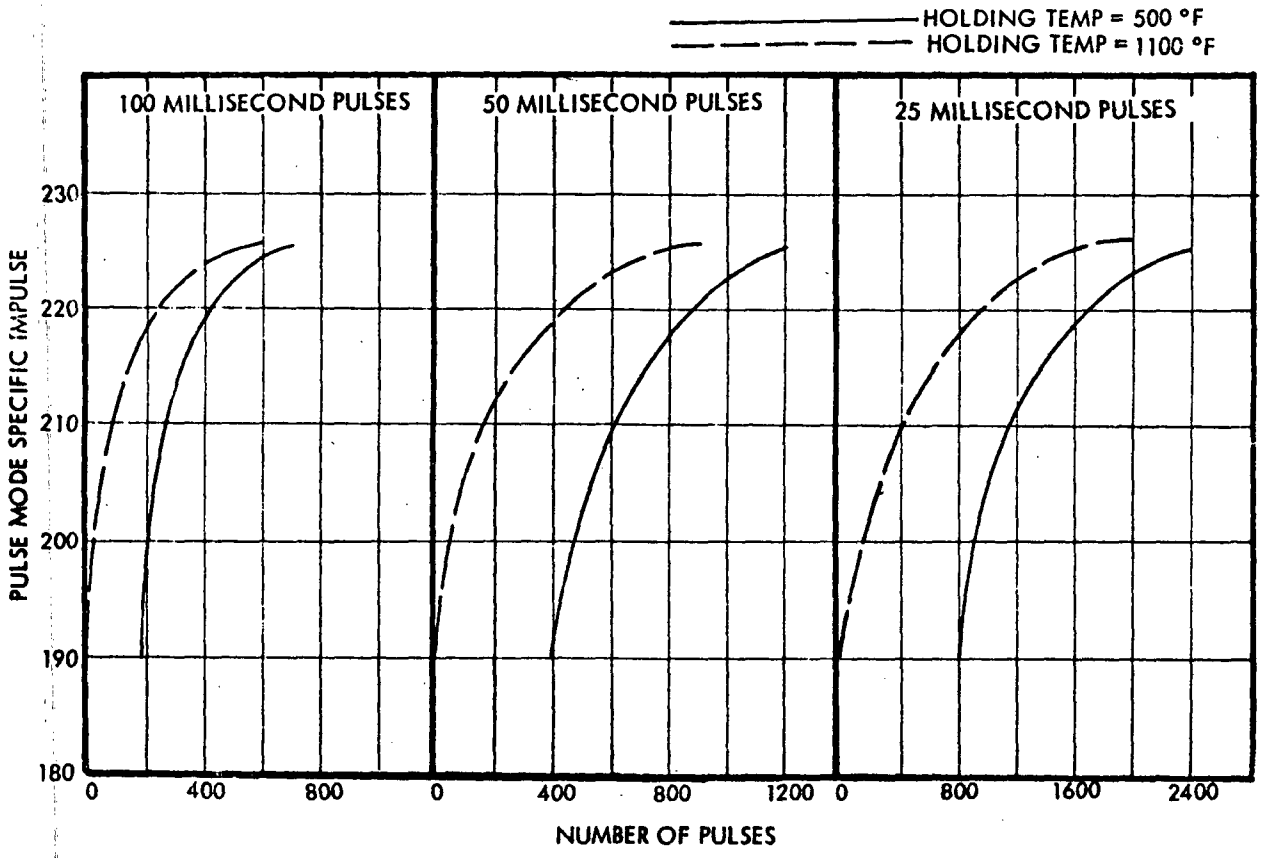

Figure 3-20a PULSE MODE SPECIFIC IMPULSE VERSUS NUMBER OF PULSES

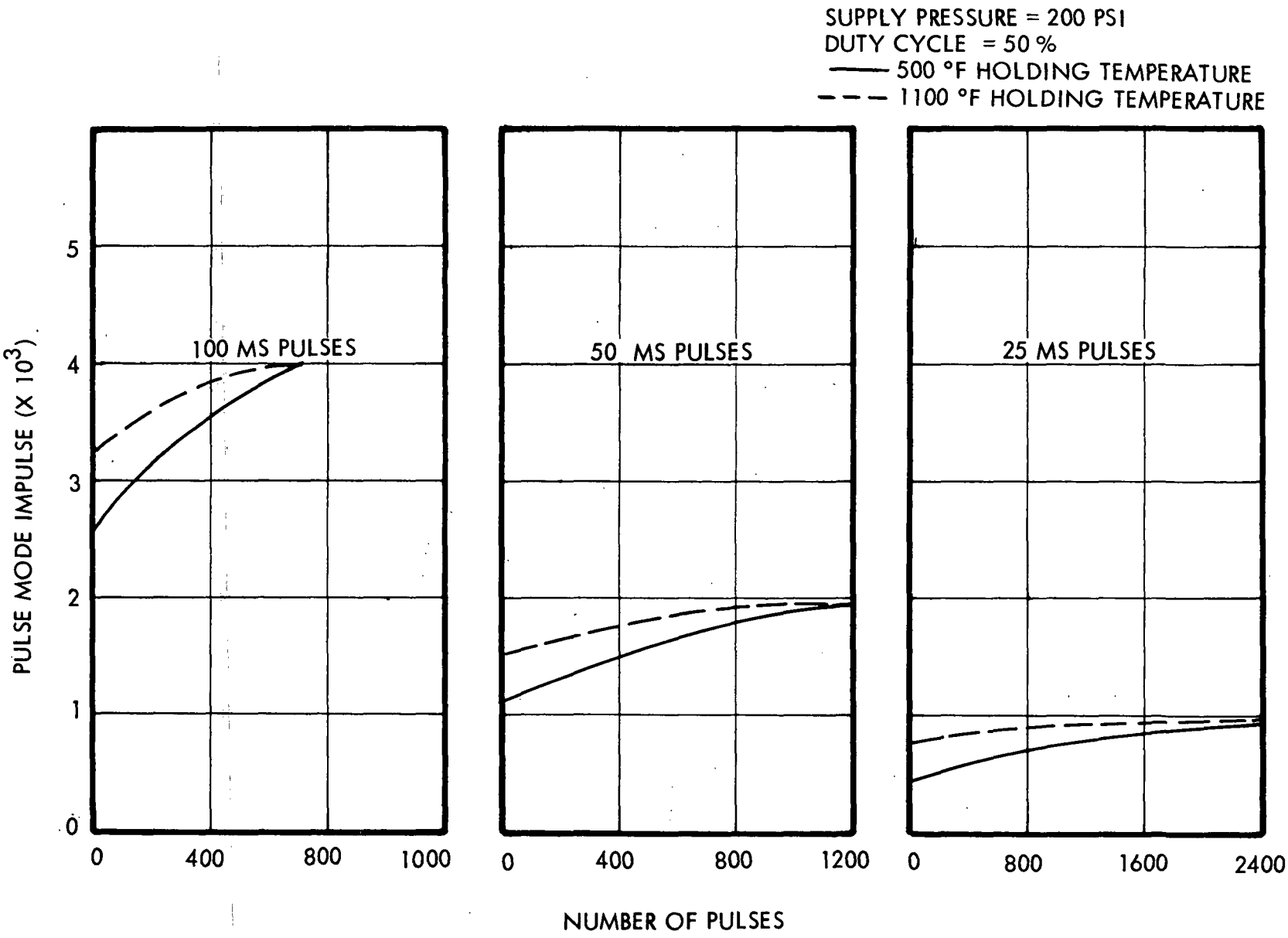

Figure 3-20b PREDICTED PULSE MODE IMPULSE BIT VERSUS NUMBER OF PULSES

due to the effective thermal capacitance. Figure 3-21, illustrates that a 50% reduction in thruster weight results in a 20-30% reduction in thruster transient rise time. Specific impulse was unaffected by variations in the thruster weight.

3.3.4 Head-End and Chamber Volume Study

Changes in thruster volumes affected the pulse mode chamber pressure rise time (Figure 3-22a) but had minimal effect on performance, as illustrated by the impulse data in Figures 3-22b and 3-22c. The pulse transient shape varies considerably with chamber volume (see computer traces in Figures 3-23 and 3-24). The net impulse bit values, however, remain relatively unchanged.

3.3.5 Chamber Wall Area

Increased thrust chamber wall area provides additional heat transfer area between the wall and gas. Negligible effects on impulse bit were shown to result from changes in this parameter (Figure 3-25). The primary effect was a reduction in rise time to steady-state with increased wall area (Figure 3-26). This data illustrates that the transient rise time to steady-state is dependent on the rate of heat transfer to the wall (which is proportional to wall area) as well as the thermal capacitance of the wall. A similar set of computer runs also showed that variations in screen pack surface area have a negligible effect on pulsed performance.

3.3.6 Injector Flow Area

The results of the injector flow area study are summarized in Figure 3-27. As expected, increased injector flow area results in reduced injector pressure drop, increased chamber pressure, and hence, increased impulse.

3.3.7 Nozzle Thrust Coefficient

Since (in the analog study) the nozzle thrust coefficient was defined as an imput parameter, a series of computer runs was made to evaluate the sensitivity of performance to thrust coefficients. Performance of this thruster under ambient atmospheric conditions may be inferred from the data of Figures 3-28a and 3-28b, since under ambient conditions the effective C_f for an expansion ratio of 50:1 is within the range of .85 to 1.0.

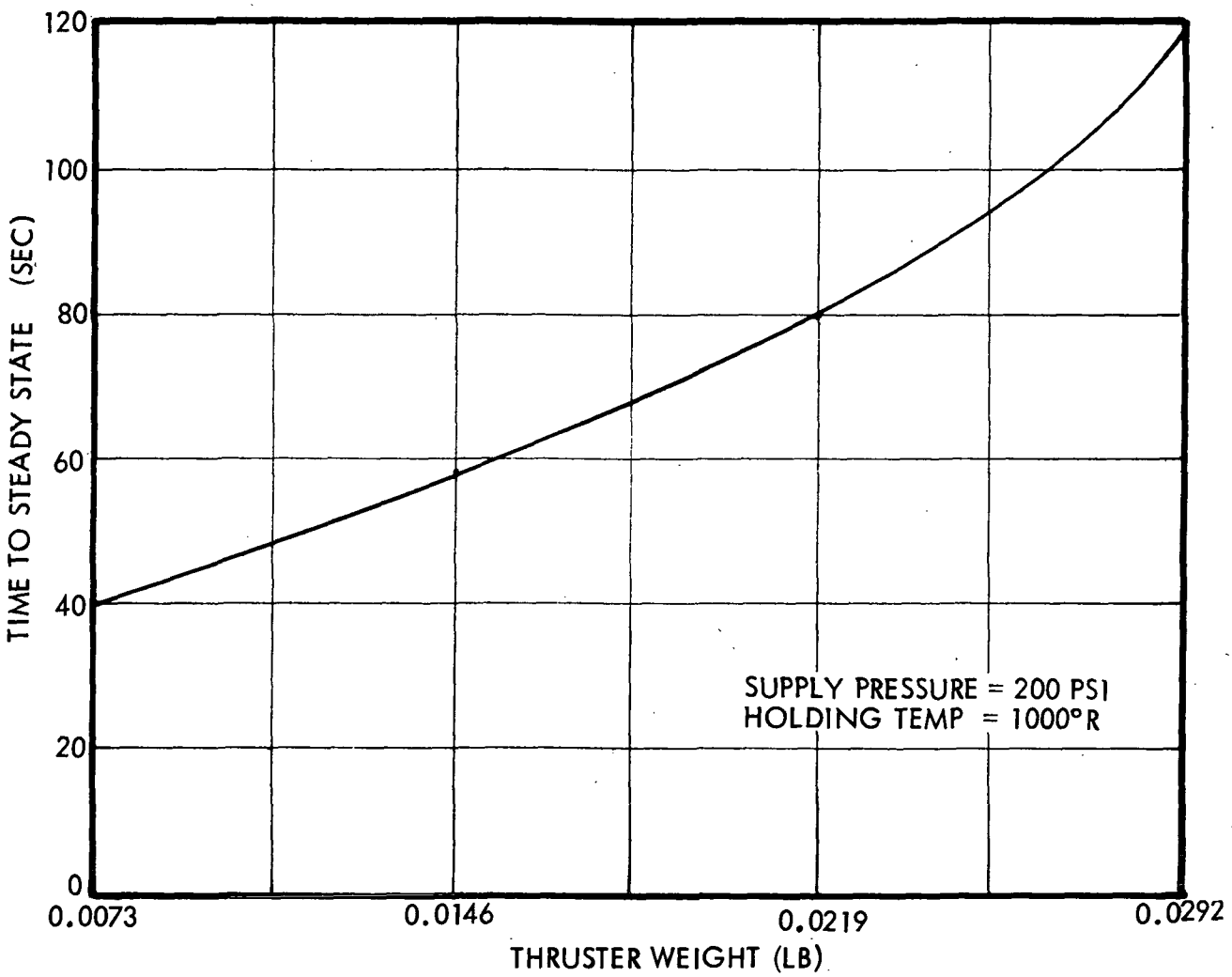

Figure 3-21 STARTUP RISE TIME REQUIRED TO REACH STEADY STATE CONDITIONS VERSUS THRUSTER WEIGHT

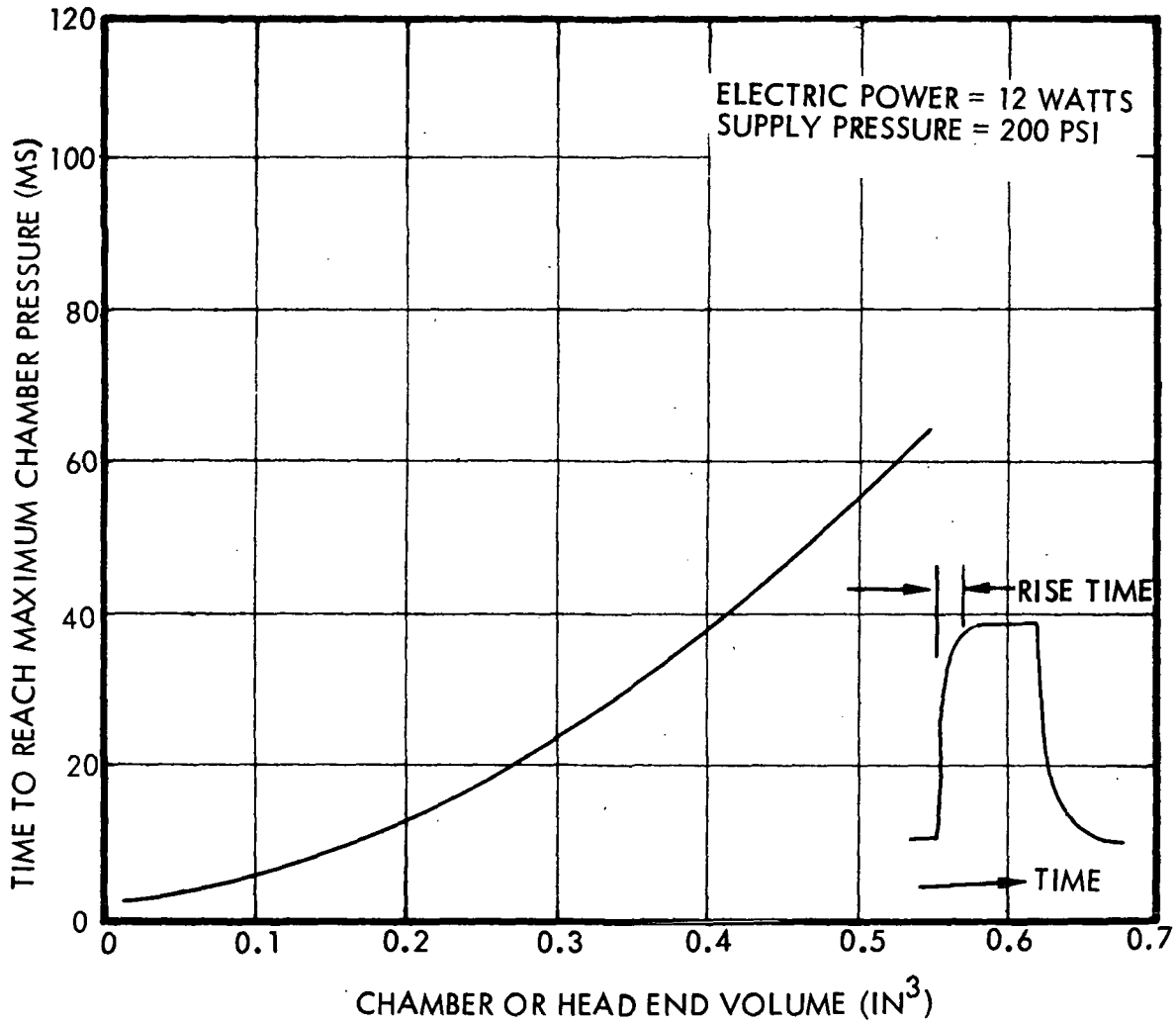

Figure 3-22a PULSE MODE TRANSIENT RISE TIME TO FULL THRUST VERSUS THRUSTER HEAD END AND CHAMBER VOLUME

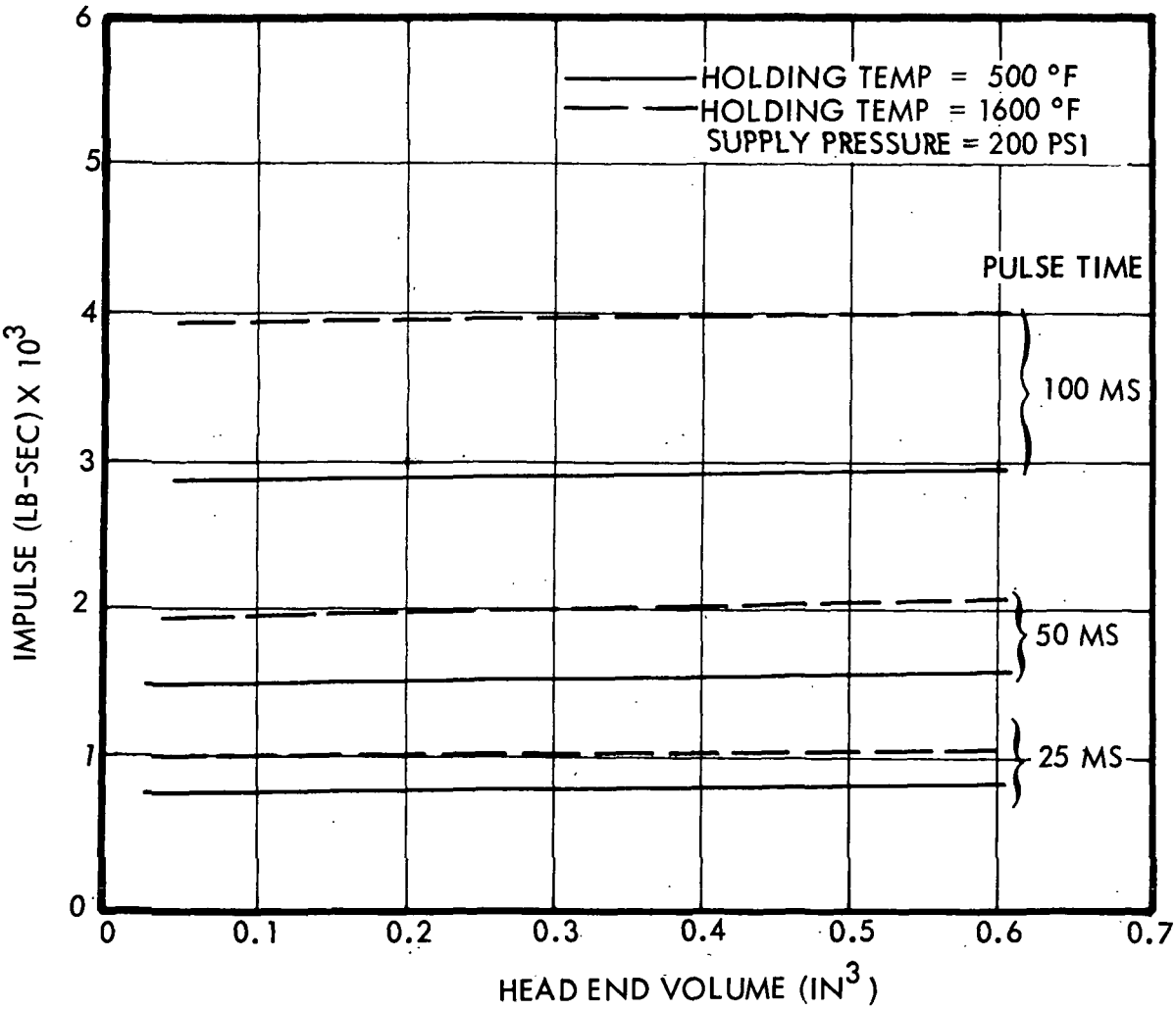

Figure 3-22b PULSE MODE IMPULSE BIT VERSUS THRUSTER HEAD END VOLUME AND WALL TEMPERATURE

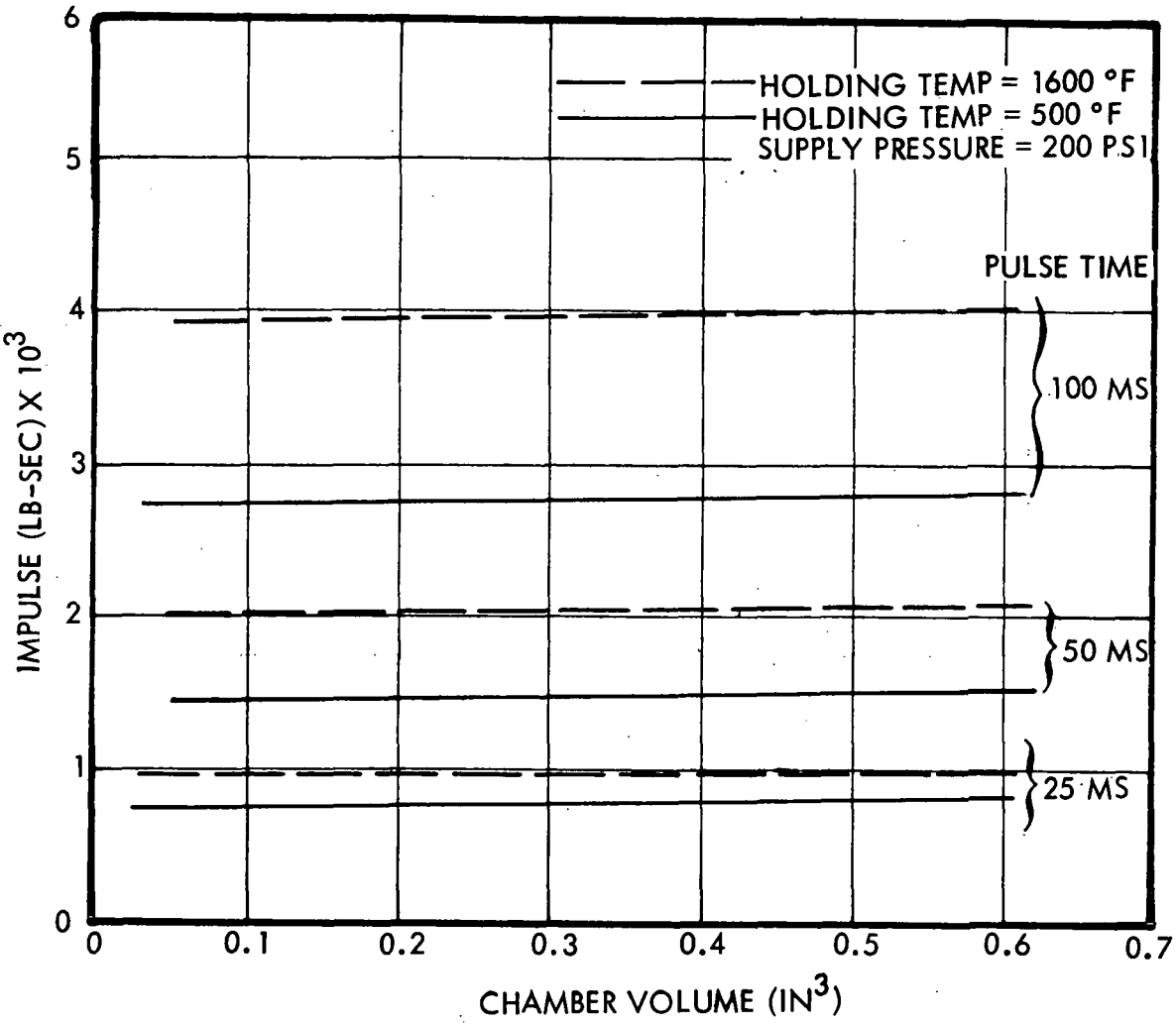

Figure 3-22c PULSE MODE IMPULSE BIT VERSUS THRUSTER CHAMBER VOLUME AND TEMPERATURE

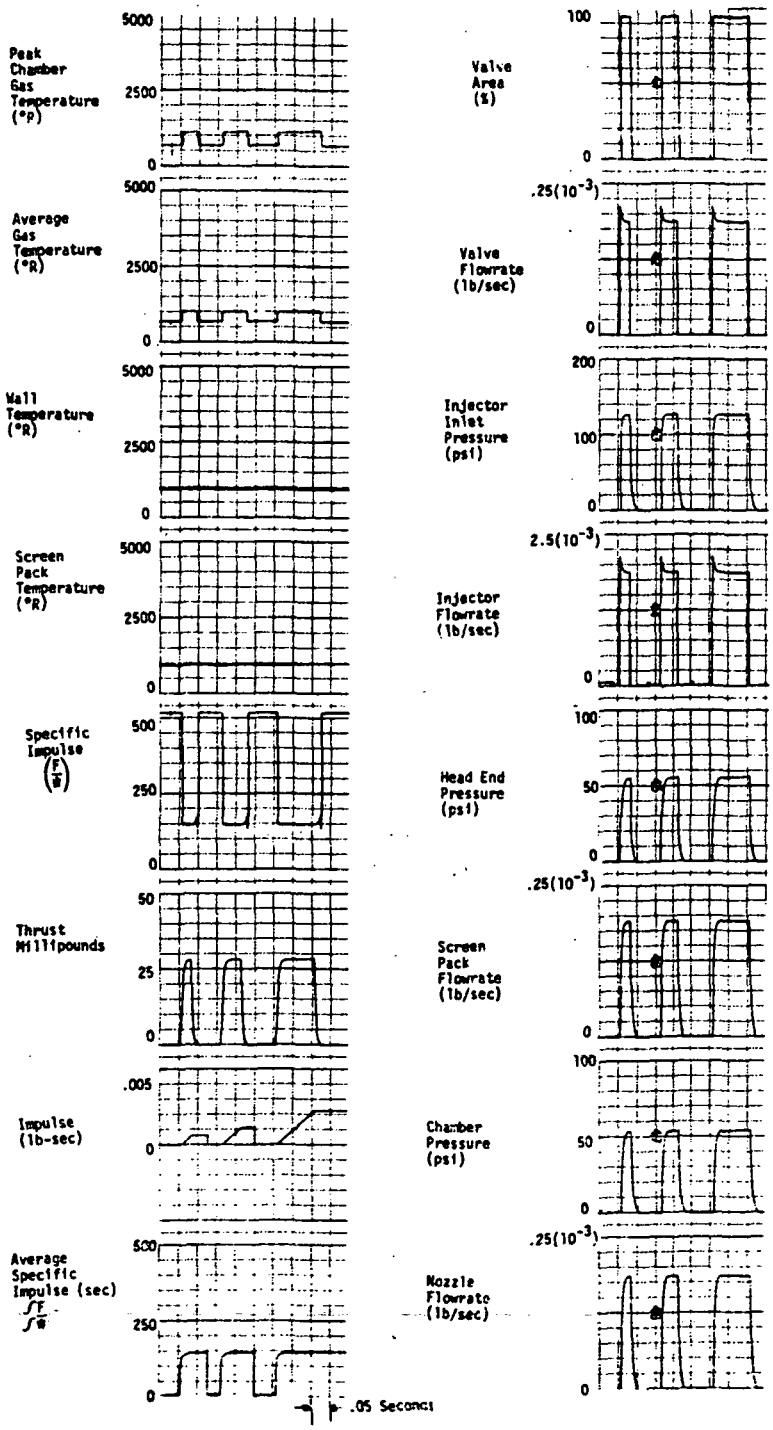

Figure 3-23 ANALOG COMPUTER TRANSIENT PERFORMANCE DATA -- CHAMBER VOLUME STUDY (VOLUME = 0.06 IN^3) (SUPPLY PRESSURE = 200 PSI, HOLDING TEMP. = 500°F)

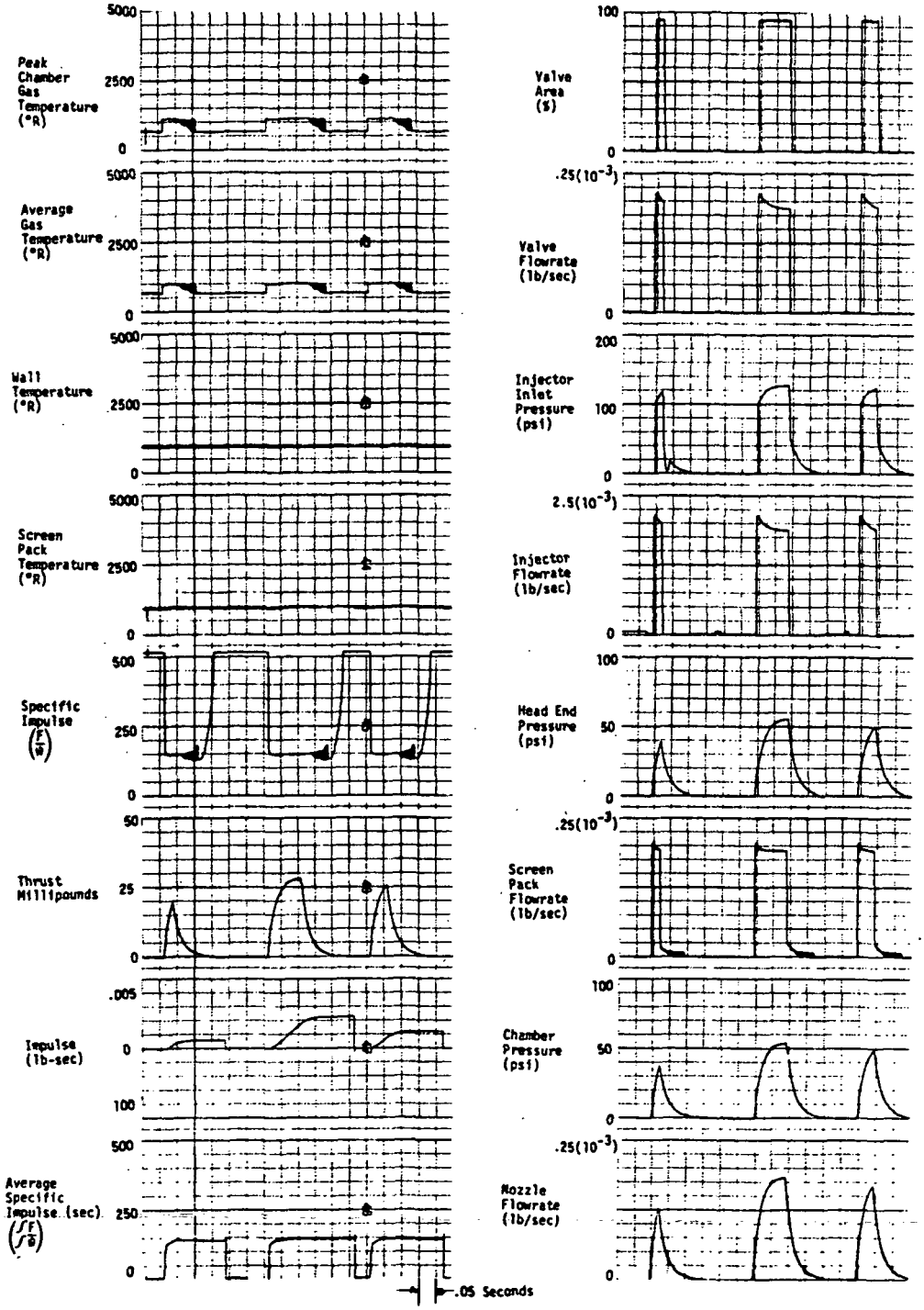

Figure 3-24 ANALOG COMPUTER TRANSIENT PERFORMANCE DATA -- CHAMBER VOLUME STUDY (VOLUME = 0.7 IN^3) (SUPPLY PRESSURE = 200 PSI, HOLDING TEMP. = 500°F)

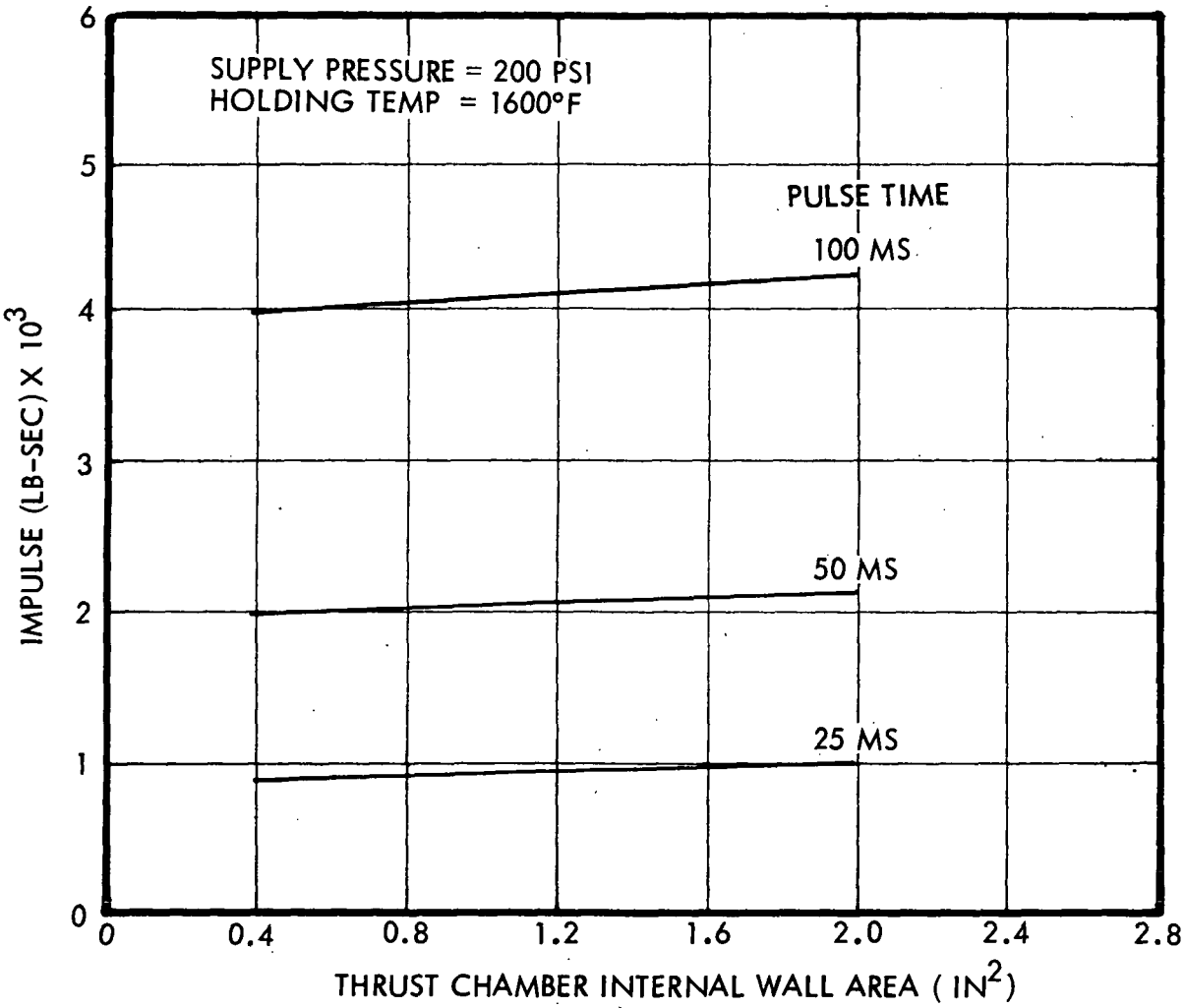

Figure 3-25 PULSE MODE IMPULSE BIT VERSUS INTERNAL CHAMBER WALL AREA

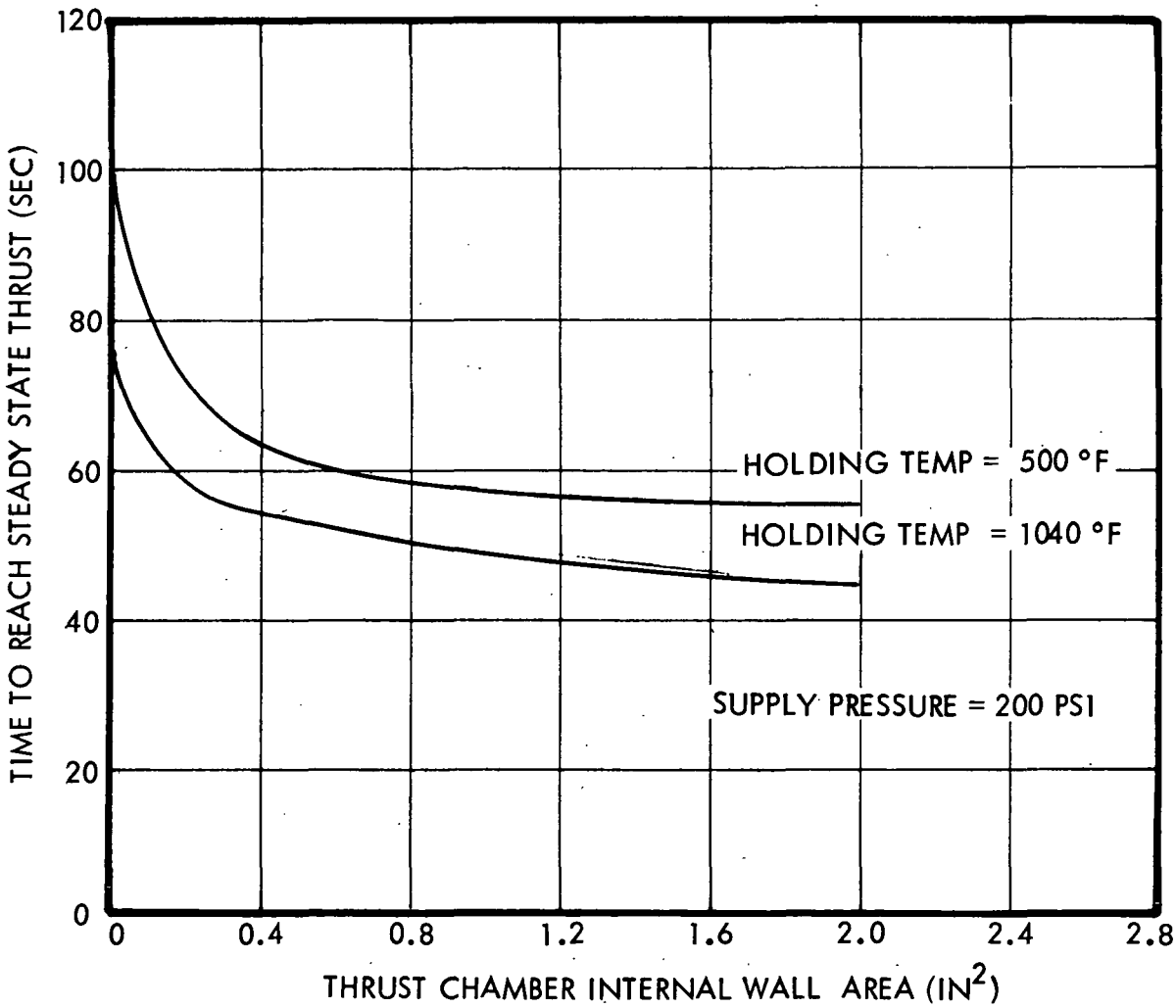

Figure 3-26 STARTUP RISE TIME REQUIRED TO REACH STEADY STATE OPERATION VERSUS INTERNAL THRUST CHAMBER WALL AREA

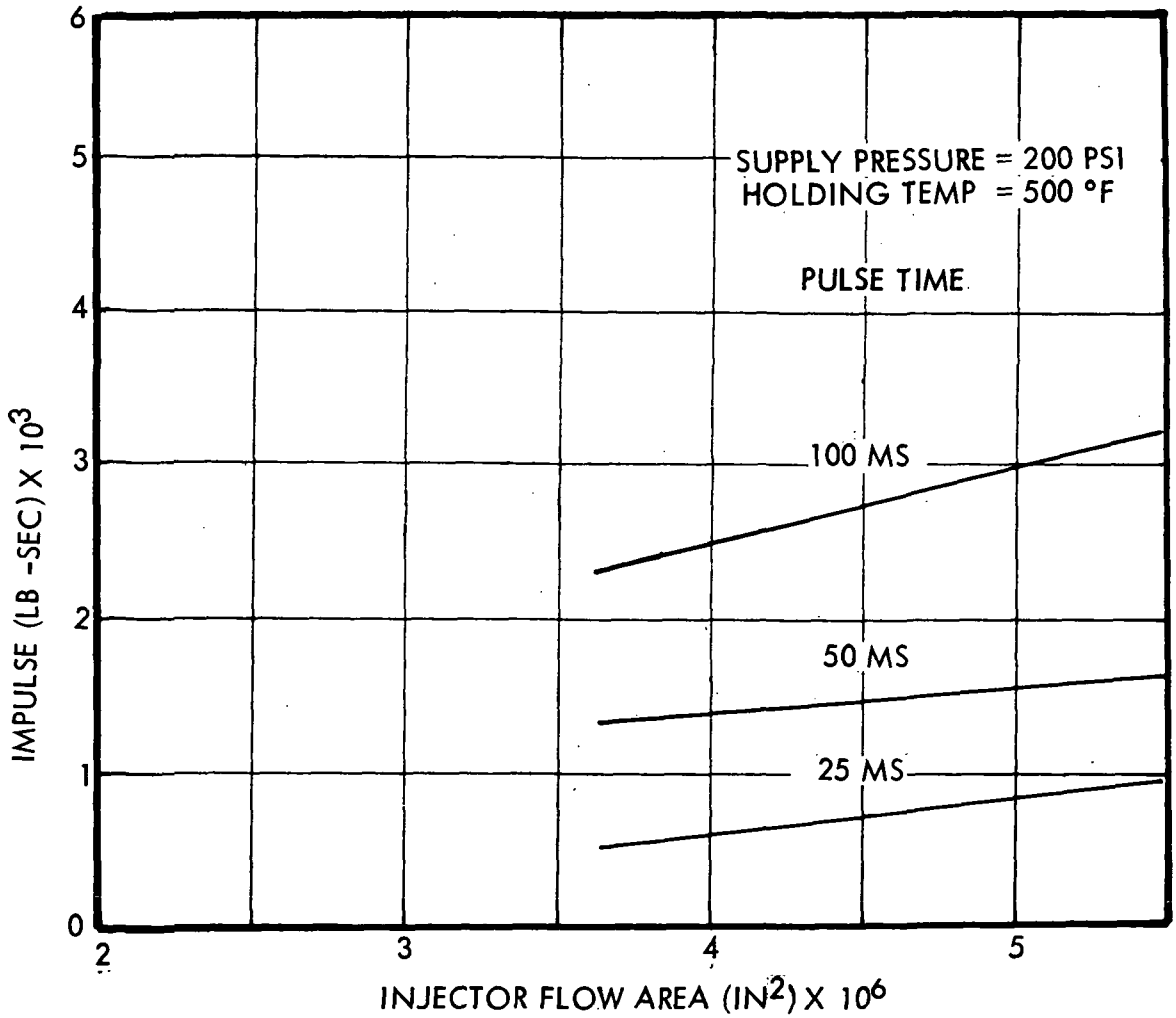

Figure 3-27 PULSE MODE IMPULSE BIT VERSUS INJECTOR FLOW AREA

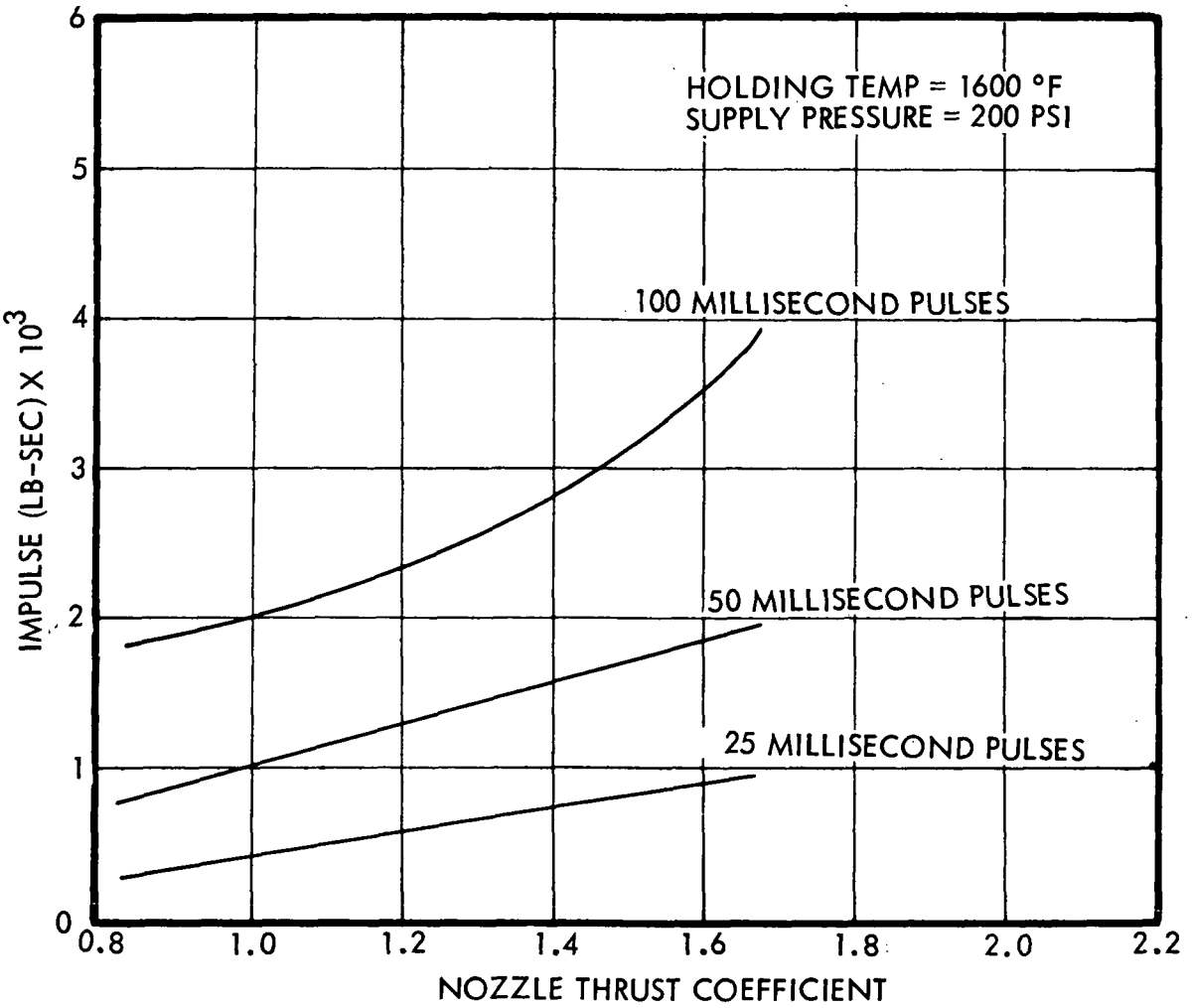

Figure 3-28a PULSE MODE IMPULSE BIT VERSUS NOZZLE THRUST COEFFICIENT

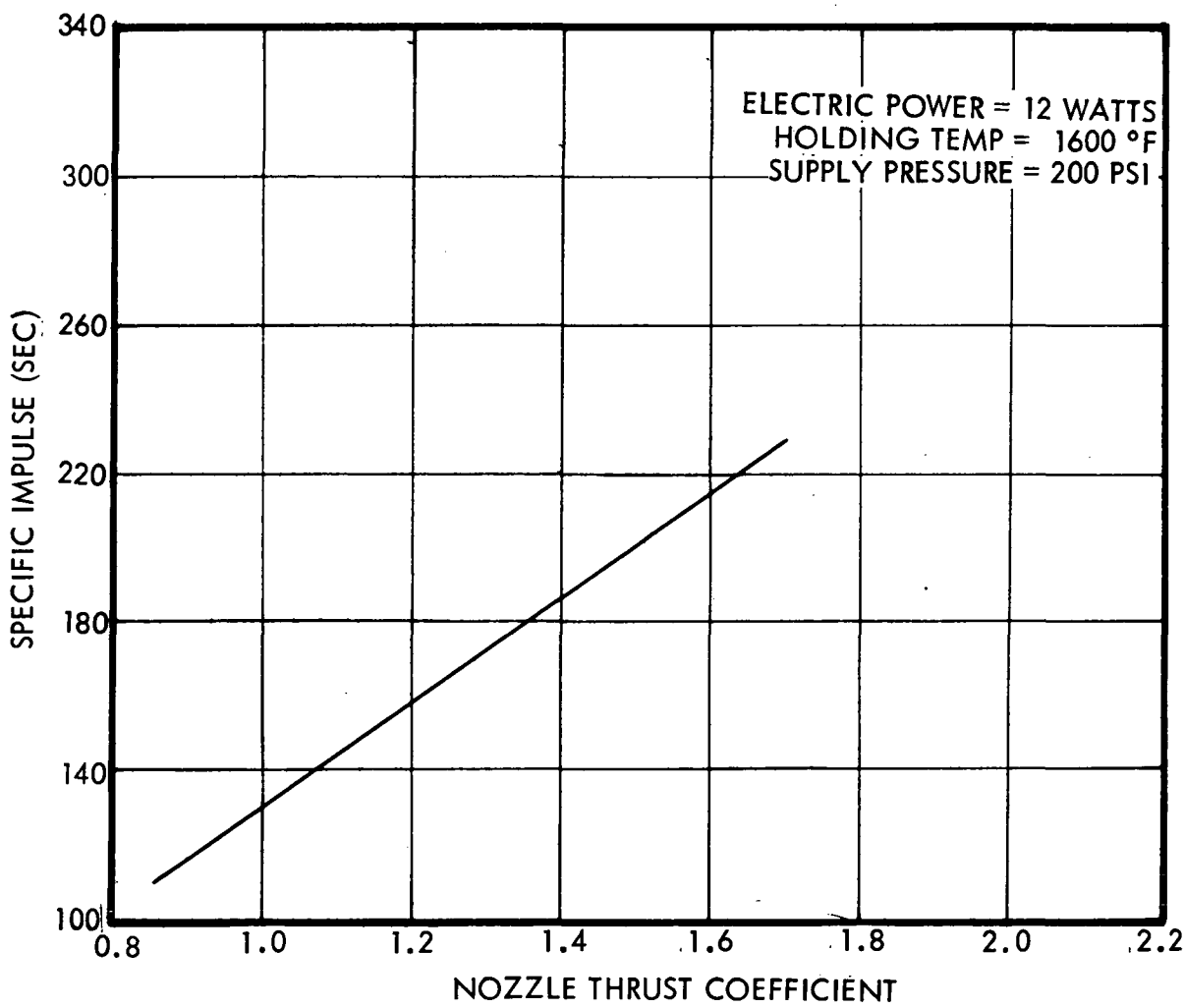

Figure 3-28b PULSE MODE SPECIFIC IMPULSE VERSUS NOZZLE THRUST COEFFICIENT

3.3.8 *Electrical Power*

Studies indicated that pulse mode transients are relatively insensitive to electrical power, the only noticable transient effect being in the rise time to steady-state. These data are summarized in Figure 3-29.

3.4 STUDY SUMMARY

While numerous computer parameter studies were conducted, not all parameter variations resulted in any significant change in performance and, therefore, not all data were plotted. For general information, a summary of all parameters considered is included in Tables 1 and 2.

TABLE I - STEADY STATE COMPUTER STUDIES*

Parameter Varied	Variation Range of Parameter	Effect on Specific Impulse	Effect on Thrust	Effect on Characteristic Velocity	Effect on C_f	Data Plotted
Supply Pressure	250-100 psi	See Figure 3-3	See Figure 3-1	See Figure 3-5	-	X
Electrical Power	0-120 watts	See Figure 3-4	See Figure 3-1	See Figure 3-5	-	X
Percent Dissociation	.2 - .7	See Figure 3-7	See Figure 3-6	See Figure 3-8	X=.2, C_f= 1.67 X=.7, C_f=1.57	X
Thruster Wall Area	± 100%	-	-	-	-	
Injector Area	± 10%	See Figure 3-12	See Figure 3-12	-	-	X
Thermal Losses	0-15 watts	See Figure 3-10	See Figure 3-9	See Figure 3-11	-	X

*Note - A dash (-) indicates negligible effect

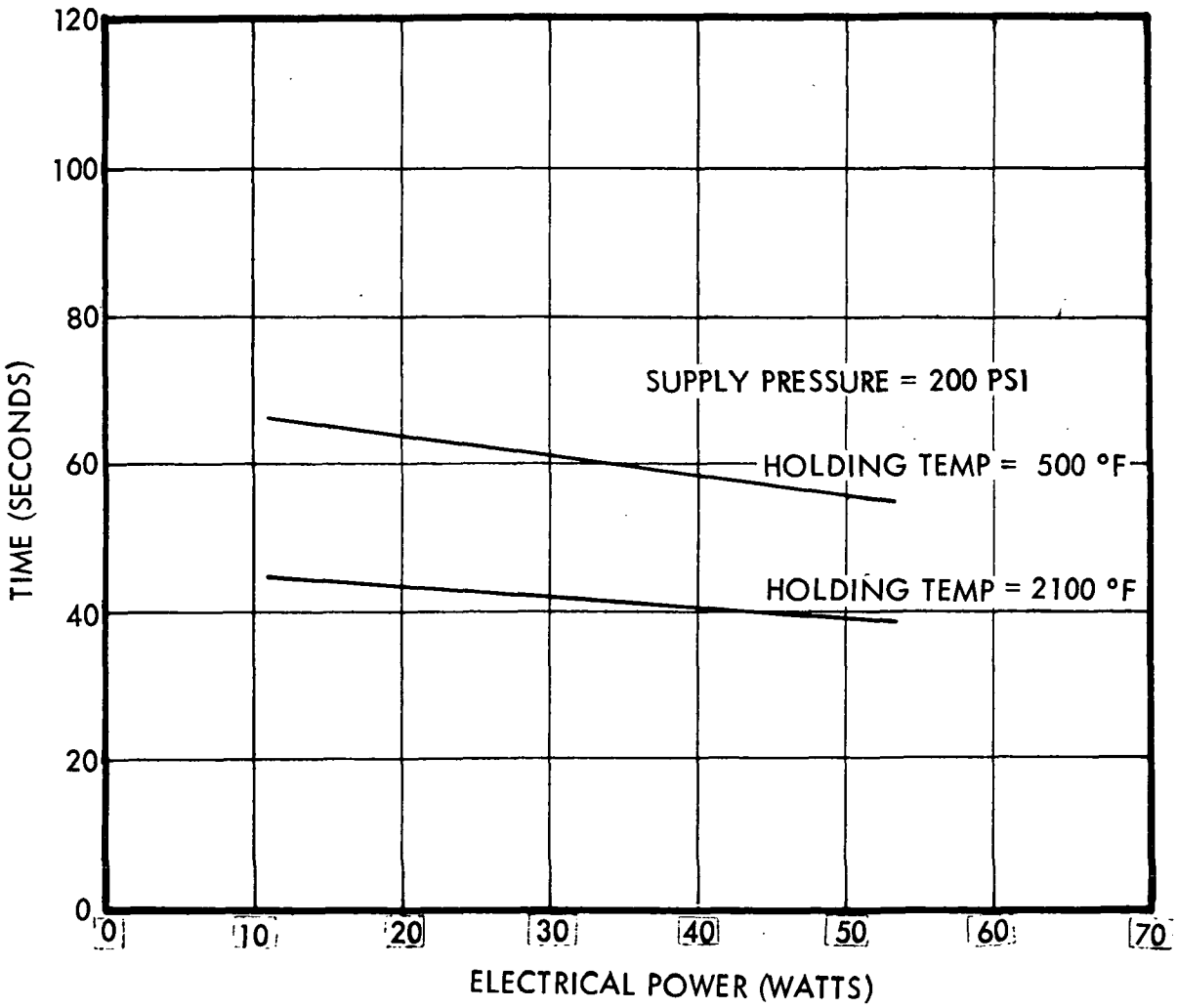

Figure 3-29 STARTUP RISE TIME REQUIRED TO REACH STEADY STATE OPERATION VERSUS ELECTRICAL POWER

TABLE II - TRANSIENT COMPUTER STUDIES

Parameter Varied	Variation Range of Parameter	Effect on Pulse Mode Impulse	Effect on Pulse Mode I_{sp}	Effect on Time to Steady-State	Data Plotted
Chamber wall Area	+ 100% - 100%	See Figure 3-25	-	See Figure 3-26	X
Screen Pack Area	+ 100% - 100%	Not Run	-	-	
Head-End Volume	+ 1000% - 30%	See Figure 3-22	-	-	X
Valve Response Time	± 100%	Proportional to valve rate	-	-	
Valve Area	± 10%	Approx. ± 10% proportional to Area	-	-	
Injector Area	± 10%	See Figure 3-27	-	-	X
Throat Area	± 10%	Approx. ± 10% proportional to Area	-	-	
Electrical Power	± 500%	-	-	See Figure 3-29	X
Supply Pressure	250-100 psi	See Figures 3-15, 3-19	See Figure 3-19	See Figures 3-14, 3-19	X
Holding Temperature	500°F-2500°F	See Figure 3-16	See Figures 3-17,3-18	See Figure 3-14	X
Dissociation Fraction	.2-.7	-	-	-	
Thruster Weight	± 100%	-	-	See Figure 3-21	X
Screen Pack Mass	± 100%	-	-	-	
Nozzle Thrust Coefficient	-50%	See Figure 3-28a,b	See Figure 3-28a,b	Not Run	X
Duty Cycle	Repeated Pulses (10% duty cycle)	See Figure 3-16	See Figure 3-20a,b	-	X

4.0 CONCLUSIONS

4.1 Performance

The Electrothermal Hydrazine Thruster Analysis Program has provided two operational computer simulation programs which have been used to characterize the steady-state and transient (pulse mode) characteristics of the thruster. These studies provide preliminary evaluation of thruster operating limits and design sensitivity. Additionally, when operating data become available, the models may be used to aid in the evaluation of test data as well as to provide supplementary data.

Results of the preliminary thruster studies are discussed in Section 3.0. The general conclusions which may be inferred from this data are:

- For the parameters evaluated, steady-state performance (specific impulse, thrust and characteristic velocity) is primarily dependent on supply pressure and electrical power.

- Pulse mode performance (impulse bit, thrust and specific impulse) is primarily dependent on thruster wall temperature (holding temperature in the case of the first pulse) and supply pressure.

4.2 Additional Areas

The models presented in this report represent comprehensive analytical tools which will prove useful in the areas of thruster design and data analysis. Potential analytical improvements which would further enhance the operation of these programs, but which are considered beyond the scope of the analysis task, are:

- More detailed characterization of the thruster insulation/thermal loss characteristics to aid in the evaluation of insulation effects.
- More detailed nozzle loss calculations to improve nozzle thrust coefficient predictions.
- More detailed characterization of the head-end/injector heat transfer characteristics to aid in the evaluation of vaporization effects in the injector tube.

Additionally, the models presented here were formulated to provide steady-state and pulse mode performance information under specific operating and configurational conditions. However, due to computer run-time limitations, the programs are not well suited to running complete duty cycle simulations. Thus, a program which would usefully compliment the existing performance programs would be a digital duty cycle evaluation program. This program would utilize data generated by the performance programs (such as wall temperature increase per pulse, wall temperature decrease as a function of off time, thermal rise time to steady-state, and flowrate per pulse) and would be used to calculate parameters such as: the number of pulses required to reach specified thrust and specific impulse (for a specified duty cycle), total propellant utilization per duty cycle, and total impulse per pulse train.

5.0 APPENDIX

5.1 Energy Balance Program

```
00110        PROGRAM FRANK(INPUT,OUTPUT,TAPE5=INPUT,TAPE6=OUTPUT)
00120        DIMENSION GAMMAT(6),CPT(6),TVT(6),HT(6),XT(6),PCT(6)
00130        DATA XT/0.,.2,.4,.6,.8,1./
00140        DATA PCT/.2,6.,10.,20.,45.,100./
00150        DATA GAMMAT/1.156,1.193,1.233,1.277,1.325,1.375/
00160        DATA CPT/.765,.7425,.7195,.7,.688,.682/
00170        DATA TVT/527.,645.,680.,715.,765.,820./
00180        DATA HT/700.,530.,510.,475.,400.,260./
00185        DATA PC,QDOT1,X,QDOTL,AN,TC1,T1,CF,KV/50.,0.,.3,
00187       +0.,3.14E-4,2337.,530.,1.65,0/
00190        NAMELIST /IC/ PC,QDOT1,X,QDOTL,AN,TC1,T1,CF,KV
00200        REAL ISP
00210        KI=1
00220  10    READ(5,IC)
00230        QDOT1=QDOT1*.0009486
00240        QDOTL=QDOTL*.0009486
00260        CALL INTERP(XT,GAMMAT,X,GAMMA,KI)
00270        CALL INTERP(XT,CPT,X,CP,KI)
00280        CALL INTERP(PCT,TVT,PC,TV,KI)
00290        CALL INTERP(PCT,HT,PC,H,KI)
00300        R=778.*((GAMMA-1.)*CP/GAMMA)
00310        FGAMMA=SQRT(32.2*GAMMA*(2./(GAMMA+1.))**((GAMMA+1.)
00320       +/(GAMMA-1.)))
00330  20    WDOT=AN*PC*FGAMMA/SQRT(R*TC1)
00340        QDOTC=1505.*WDOT
00350        QDOTV=(CP*(TV-T1)+H)*WDOT
00355        IF(KV.LT.1) QDOTV=0.
00360        QDOTD=825.*X*WDOT
00370        DELT=(QDOTC-QDOTV-QDOTD-QDOTL+QDOT1)/CP/WDOT
00380        TC=TV+DELT
00390        IF(ABS(TC-TC1).LE.1.) GO TO 50
00400        TC1=TC1+(TC-TC1)/2.
00420        GO TO 20
00460  50    ISP=CF*SQRT(R*TC1)/FGAMMA
00510        QD1=QDOT1/.0009486
00520        QDC=QDOTC/.0009486
00530        QDV=QDOTV/.0009486
00540        QDD=QDOTD/.0009486
00550        QDL=QDOTL/.0009486
00555        F=ISP*WDOT
00560        WRITE(6,1000) PC,AN,TC,T1,WDOT,ISP,F
00570 1000   FORMAT(//,5X,21HCHAMBER PRESSURE     =E11.3,2X,4HPSIA/
```

```
00580       +5X,11HTHROAT AREA,9X,1H=E11.3,2X,
00590       +13HINCHES SQUARE/5X,21HCHAMBER TEMPERATURE =E11.3,
00600       +2X,9HDEGREES R/5X,21HINLET TEMPERATURE    =E11.3,
00610       +2X,9HDEGREES R/5X,8HFLOWRATE,12X,1H=E11.3,2X,
00620       +9HLBS./SEC./5X,21HSPECIFIC IMPULSE     =E11.3,
00630       +2X,4HSEC./5X,6HTHRUST,14X,1H=E11.3,2X,6HLBS.-F/)
00660        WRITE(6,1100) QDOTI,QDI,QDOTC,QDC,QDOTV,QDV,QDOTD,
00670       +QDD,QDOTL,QDL
00680 1100   FORMAT(22X,7HBTU/SEC,6X,5HWATTS/2X,
00690       +18HELECTRICAL INPUT =E11.3,2X,E11.3/2X,
00700       +18HDECOMPOSITION    =E11.3,2X,E11.3/2X,
00710       +18HVAPORIZATION     =E11.3,2X,E11.3/2X,
00720       +18HDISSOCIATION     =E11.3,2X,E11.3/2X,6HLOSSES,
00730       +11X,1H=E11.3,2X,E11.3//)
00740        QDOTI=QDOTI/.0009486
00750        QDOTL=QDOTL/.0009486
00770        GO TO 10
00780        END
00790        SUBROUTINE INTERP(XI,YI,X,Y,KI)
00800        DIMENSION XI(6),YI(6)
00810        IF(KI.LE.1) KI=2
00820        IF(X-XI(KI)) 10,20,30
00830 10     IF(X-XI(KI-1)) 40,50,60
00840 40     IF(X.GT.XI(1)) GO TO 70
00850        Y=YI(1)
00860        KI=2
00870        RETURN
00880 70     KI=KI-1
00890        IF(KI.LE.2) GO TO 60
00900        IF(X-XI(KI)) 70,20,60
00910 20     Y=YI(KI)
00920        RETURN
00930 30     IF(X.LT.XI(6)) GO TO 80
00940        Y=YI(6)
00950        KI=6
00960        RETURN
00970 50     Y=YI(KI-1)
00980        KI=KI-1
00990        RETURN
01000 80     DO 90 KI=KI,6
01010        ERR=X-XI(KI)
01020        IF(ERR) 60,20,90
01030 90     CONTINUE
01040 60     Y=YI(KI-1)+((YI(KI)-YI(KI-1))*(X-XI(KI-1))/(XI(KI)
01050       +-XI(KI-1)))
01060        RETURN
01070        END
```

5.2 Steady-State Performance Program

```
00100       PROGRAM RESISTO(INPUT,OUTPUT,TAPE5=INPUT,TAPE6=OUTPUT)
00110       DIMENSION PVTAB(11),TFTAB(11),RRTAB(11),XXTAB(11)
00120       DIMENSION CPTAB(11),GAMTAB(11),QDLTAB(11),TWTAB(11)
00130       REAL K1,ISP
00140       NAMELIST /DATA/ AVOPEN,PVTAB,TFTAB,CD,RHOL,AI,U,A2,
00150      +K1,R,XXTAB,CSTAB,AT,H,FO,QD1,X,AW,AS,PO,T1,ETA,PA
00160       DATA AVOPEN,CD,AI,RHOL,U,A2/4.27E-6,1.,4.48E-6,.035,
00170      +2.24E-3,.07/
00180       DATA K1,R,AT,H/1.7E-2,1212.,3.14E-4,5.7373/
00190       DATA PVTAB  /.2,.6,1.,2.,7.,20.,42.,100.,170.,450./
00200       DATA TFTAB  /70.,100.,120.,140.,200.,250.,300.,360.,400.,500.
00210       DATA X,PO,T1,QD1/.3,200.,530.,12./
00220       DATA XXTAB /0.,.15,.3,.45,.65,.9,1./
00230       DATA RRTAB /970.6,1050.,1200.,1310.,1476.,1644.,1716./
00240       DATA CPTAB/.765,.748,.731,.714,.696,.6845,.682/
00250       DATA GAMTAB/1.157,1.188,1.213,1.245,1.29,1.35,1.375/
00260       DATA QDLTAB/.25,.6,1.05,1.8,2.7,5.0,7.6/
00270       DATA TWTAB/600.,800.,1000.,1250.,1500.,2000.,2500./
00280       DATA AW,AS,FO,ETA,PA/.2,.7,50.,.876,0./
00290  50   READ(5,DATA)
00300       QDOT1=QD1*.0009486
00310       QDOTL=5.0*.0009486
00320       WCHEK=1.E6
00330       XIT=50.
00340       AX=U*A2
00350       KOUNT=0
00360       T3=2300.
00370       WDOT=1.E-4
00380       CP=XINT(X,XXTAB,CPTAB,7)
00390       CO=CD*AVOPEN*SQRT(2.*386.*RHOL)
00400       C1=CD*AI*SQRT(2.*386.*RHOL)
00410       R=XINT(X,XXTAB,RRTAB,7)
00420  20   CONTINUE
00430       BX1=H*AW*WDOT**.8
00440       BX2=H*AS*WDOT**.8
00450  80   TW=(QDOT1-QDOTL+T3*(BX1+AX*BX2/(BX2+AX)))/(AX-AX**2
00460      +/(BX2+AX)+BX1)
00470       TS=(AX*TW+BX2*T3)/(BX2+AX)
00480       QDOT2=(TW-TS)*AX
00490       QDOT3=(TW-T3)*BX1
00500       QDOT4=(TS-T3)*BX2
00510       QDOTO=(1505.-825.*X)*WDOT
```

```
00520          TDEL=(QDOT0+QDOT3+QDOT4)/CP/WDOT
00530          T2=XINT(PC,PVTAB,TFTAB,10)+460.
00540          T3N=T2+TDEL/1.4
00550          TC=T2+TDEL
00560          IF(ABS(T3/T3N-1.).LT.0.01) GO TO 90
00570          T3=T3N+(T3-T3N)/2.
00580          QDOTL=XINT(TW,TWTAB,QDLTAB,7)*.0009486
00590          KOUNT=KOUNT+1
00600          IF(KOUNT.GT.500) GO TO 10
00610          GO TO 80
00620 90       CONTINUE
00630          P1=P0-(WDOT/C0)**2
00640          P2=P1-(WDOT/C1)**2
00650          GAM=XINT(X,XXTAB,GAMTAB,7)
00660          CS1=SQRT(32.2*GAM*(R/12.)*TC)
00670          CS2=(2./(GAM+1.))**((GAM+1.)/(GAM-1.))
00680          CS3=GAM*SQRT(CS2)
00690          CSTAR=CS1/CS3
00700          C3=32.2*AT/CSTAR
00710          PC=WDOT/C3
00720          P3=(P2+PC)/2.
00730          C2=K1*SQRT(1./R/T3)
00740          WDOTN=C2*SQRT(P3*(P2-PC))
00750          DELW=WDOTN-WDOT
00760          IF(ABS(WDOT/WDOTN-1.).LT.0.001) GO TO 10
00770          IF(ABS(DELW).GT.WCHEK) XIT=XIT*2.
00780          WDOT=WDOT+(WDOTN-WDOT)/XIT
00790          WCHEK=ABS(DELW)
00800          KOUNT=KOUNT+1
00810          IF(KOUNT.GT.500) GO TO 10
00820          GO TO 20
00830 10       CONTINUE
00840          IF(KOUNT.GE.500) WRITE(6,1400) KOUNT,XIT
00850 1400     FORMAT(2X,6HKOUNT=I5,2X,4HXIT=E10.3)
00860          T2W=T2-460.
00870          T3W=T3-460.
00880          TSW=TS-460.
00890          TWW=TW-460.
00900          TCW=TC-460.
00910          T1W=T1-460.
00920          QD0=QDOT0/.0009486
00930          QD2=QDOT2/.0009486
```

```
C0940         QD3=QDOT3/.0009486
00950         QD4=QDOT4/.0009486
00960         QDL=QDOTL/.0009486
00970         GAM=XINT(X,XXTAB,GAMTAB,7)
00980         CALL CSUBF(GAM,FO,CF,ETA,PA,PC)
00990         F=PC*AT*CF
01000         ISP=F/WDOT
01010         WRITE(6,900) PO,T1W,QD1,X,AI,AT,FO
01020   900   FORMAT(20X,12H***INPUTS***//5X,15HSUPPLY PRESSURE,8X,
01030        +1H=E11.3,2X,4HPSIA/5X,18HSUPPLY TEMPERATURE,5X,1H=E11.3,
01040        +2X,9HDEGREES F/5X,24HELECTRICAL POWER INPUT =E11.3,2X,
01050        +5HWATTS/5X,24HDISSOCIATION FRACTION  =E11.3/5X,
01060        +13HINJECTOR AREA,10X,1H=E11.3,2X,13HSQUARE INCHES/5X,
01070        +11HTHROAT AREA,12X,1H=E11.3,2X,13HSQUARE INCHES/
01080        +5X,15HEXPANSION RATIO,8X,1H=E11.3/)
01090         WRITE(6,1000)     P1,P2,P3,PC
01100         WRITE(6,1100) T2W,T3W,TSW,TWW,TCW
01110         WRITE(6,1200) QD0,QD2,QD3,QD4,QDL
01120         WRITE(6,1300) CF,WDOT,F,ISP,CSTAR
01130  1000   FORMAT(20X,12H---OUTPUT---//
01140        +5X,23HINJECTOR INLET PRESSURE,6X,1H=E11.3,2X,4HPSIA/
01150        +5X,17HHEAD END PRESSURE,12X,1H=E11.3,2X,4HPSIA/5X,
01160        +30HAVERAGE SCREEN PACK PRESSURE =E11.3,2X,4HPSIA/
01170        +5X,16HCHAMBER PRESSURE,13X,1H=E11.3,2X,4HPSIA/)
01180  1100   FORMAT(     5X,26HVAPORIZATION TEMPERATURE =E11.3,
01190        +2X,9HDEGREES F/5X,26HAVERAGE GAS TEMPERATURE  =E11.3,
01200        +2X,9HDEGREES F/5X,26HSCREEN PACK TEMPERATURE  =E11.3,
01210        +2X,9HDEGREES F/5X,16HWALL TEMPERATURE,9X,1H=E11.3,
01220        +2X,9HDEGREES F/5X,19HCHAMBER TEMPERATURE,6X,1H=E11.3,
01230        +2X,9HDEGREES F/)
01240  1200   FORMAT(5X,19HCHEMICAL HEAT INPUT,6X,1H=E11.3,2X,
01250        +5HWATTS  /5X,26HWALL TO SCREEN HEAT FLUX =E11.3,2X,
01260        +5HWATTS  /5X,21HWALL TO GAS HEAT FLUX,4X,1H=E11.3,
01270        +2X,5HWATTS  /5X,26HSCREEN TO GAS HEAT FLUX  =E11.3,
01280        +2X,5HWATTS/5X,11HHEAT LOSSES,14X,1H=E11.3,2X,5HWATTS/)
01290  1300   FORMAT(5X,20HTHRUST COEFFICIENT =E11.3/
01300        +5X,8HFLOWRATE,11X,1H=E11.3,2X,9HLBS./SEC./
01310        +5X,6HTHRUST,13X,1H=E11.3,2X,6HLBS.-F/5X,
01320        +20HSPECIFIC IMPULSE   =E11.3,2X,4HSEC./
01330        +5X,5HCSTAR,14X,1H=E11.3,2X,7HFT/SEC.//)
01340         GO TO 50
01350         END
```

```
01360       FUNCTION XINT(X,XT,YT,NT)
01370       DIMENSION XT(1),YT(1)
01380       IF(X.GT.XT(1)) GO TO 40
01390       K=2
01400       GO TO 20
01410  40   IF(X.LT.XT(NT)) GO TO 30
01420       K=NT
01430       GO TO 20
01440  30   DO 10 K=2,NT
01450       IF(X.GE.XT(K-1)  .AND. X.LE.XT(K)) GO TO 20
01460  10   CONTINUE
01470  20   RATIO=(X-XT(K-1))/(XT(K)-XT(K-1))
01480       XINT=YT(K-1)+RATIO*(YT(K)-YT(K-1))
01490       RETURN
01500       END
01510       SUBROUTINE CSUBF(GAM,F0,CF,ETA,PA,PC)
01520       DATA PRAT/.05/
01530       ICOUNT=0
01540  50   F=(2./(GAM+1.))**((GAM+1.)/(2.*(GAM-1.)))/((PRAT**(1.
01550      +/GAM))*SQRT(2./(GAM-1.)*(1.-PRAT**((GAM-1.)/GAM))))
01560       IF(ABS(F/F0-1.).LT.0.01) GO TO 100
01570       DF1=(PRAT**(1./GAM)*(-2./GAM*PRAT**(1./GAM)))*.5/
01580      +(2./(GAM-1.)*(1.-PRAT**((GAM-1.)/GAM)))
01590       DF2=SQRT((2./(GAM-1.))*(1.-PRAT**((GAM-1.)/GAM)))*
01600      +PRAT**((1.-GAM)/GAM)/GAM
01610       DF3=PRAT**(2./GAM)*2./(GAM-1.)*(1.-PRAT**((GAM-1.)/
01620      +GAM))
01630       DF4=(2./(GAM+1.))**((GAM+1.)/(2.*(GAM-1.)))
01640       DF=DF4*(DF1+DF2)/DF3
01650       PRATX=PRAT
01660       PRAT=PRAT+(F-F0)/DF
01670       IF(PRAT.LE.0.0) PRAT=PRATX/2.
01680       ICOUNT=ICOUNT+1
01690       IF(ICOUNT.GT.100) GO TO 200
01700       GO TO 50
01710 100   CF=SQRT((2.*GAM**2/(GAM-1.))*(2./(GAM+1.))**((GAM+1.)/
01720      +(GAM-1.))*(1.-PRAT**((GAM-1.)/GAM)))
01730       CF=(CF+(PRAT-(PA/PC))*F0)*ETA
01740       RETURN
01750 200   WRITE(6,2000) ICOUNT
01760 2000  FORMAT(2X,7HICOUNT=I4)
01770       RETURN
01780       END
```

5.3 REFERENCES

1. "Basic Factors Involved in the Design and Operation of Catalytic Monopropellant Hydrazine Reaction Chambers," A. F. Grant, Jr., Jet Propulsion Laboratory Report No. 20-77, December 1954

2. "Monopropellant Hydrazine Resistojet Proposal," TRW Document 20266.000, March 1971

3. AIAA Journal, January 1957, "A Simple Equation for Rapid Estimation of Rocket Nozzle Heat Transfer Coefficients," D. R. Bartz

4. "Rocket Propulsion Elements," George P. Sutton, John Wiley and Sons, 1949.